Tunable, strongly-donating perylene photosensitizers for dye-sensitized solar cells

AUTHOR(S):

Mathew, Simon; Imahori, Hiroshi

CITATION:

Mathew, Simon ...[et al]. Tunable, strongly-donating perylene photosensitizers for dye-sensitized solar cells. Journal of Materials Chemistry 2011, 21(20): 7166-7174

ISSUE DATE:

2011-04

URL:

http://hdl.handle.net/2433/156621

Tunable, Strongly-Donating Perylene Photosensitizers for Dye-Sensitized Solar Cells

Simon Mathew[a,b] and Hiroshi Imahori[*,a,b,c]

Received (in XXX, XXX) Xth XXXXXXXXX 200X, Accepted Xth XXXXXXXXX 200X
First published on the web Xth XXXXXXXXX 200X
DOI: 10.1039/b000000x

Broadly absorbing perylene dyes bearing three-triarylamine groups were synthesized via Sonogashira coupling. The triarylamine moieties allowed further installation of electron donating ability, to enable tuning of the oxidation potential and optical bandgap. With introducing more electron-donating groups into the three-triarylamine moieties the device performance was improved. The trend can be rationalized by the distribution of the electron density in the HOMO of the perylene moiety as well as the light-harvesting property of the perylene dyes.

Introduction

Dye-sensitized solar cells (DSSCs) have been actively pursued as an economical solar energy conversion technology since their inception over two decades ago.[1] The composition of a typical DSSC is a photoanode composed of conductive glass (e.g. fluorine-doped tin oxide, FTO, Figure 1) to which a layer of an inexpensive, inorganic *n*-type semiconductor is applied. In the case of the most DSSCs, nanocrystalline TiO_2 is used but the versatility of the cell allows the use of other *n*-type semiconductors (e.g. SnO_2, ZnO) and even the use of *p*-type semiconductors (NiO).[2, 3] The nanocrystalline (20 nm) nature of the TiO_2 particles imparts a large surface area to the semiconductor, a trait which enables the subtrate to adsorb large amounts of photosensitizer. Absorption of light by the dye facilitates the transition from the dye ground state (D) to the dye excited singlet state (D^*). The dye excited singlet state is able to inject this electron into the conduction band (CB) of the TiO_2 semiconductor to yield a dye radical cation ($D^{\bullet+}$). The oxidized dye returns to the neutral, ground state through recombination at the cathode with the injected electron via a redox electrolyte, in many instances I^-/I_3^-.

Figure 1. Construction and operation of a DSSC.

The nature of the photosensitizer used to harvest the light is directly related to the efficiency of the corresponding cell. To date, the use of organometallic dyes, namely heteroleptic ruthenium complexes has remained the highest performing dye component used in the DSSC.[4] However, this class of dye possesses some undesirability due to the low natural abundance (1 ppb) of the rare eath metal used. The quest to develop fully organic dyes or inexpensive metal complexes has revealed the possibilty of many types of dye to achieve high performance when used in a DSSC.[5] Of these dyes, perylene photosensitizers have been explored as possible alternatives due to their chemical and thermal stablility, low cost and excellent light-harvesting ability.[6] The physical and chemical features of perylene dyes make them ideal candidates for use as photosensitizers in DSSCs. The anhydride moiety, used to anchor the perylene to the TiO_2 can also be incorporated into the dye structure with great ease. The inclusion of the anhydride functional group is essential, as it has been shown to promote strong electronic communcation between the LUMO of the dye and the CB of TiO_2.[7-9]

The result of this enhanced electronic communication is fast electron injection from D^* to the CB of the TiO_2 and is an essential feature to realizing efficient DSSCs. At the same time, obtaining tunability of the dye properties, such as steric hindrance, redox potentials and optical properties in a controlled and simple manner, is vital in synthesizing new and efficient dyes.

One particular feature of great interest in designing dyes for application in solar cells is the ability to impart charge transfer (CT) absorption characteristics by inducing partitioning of the frontier orbitals. In perylene monoanhydrides, this can be achieved by simple substitution of an electron-donating group, usually an amine, on the 9-position of the perylene core. The perturbation of HOMO and LUMO distribution within the molecule results in localization of the frontier orbitals around the amine and anhydride functionalities respectively.[10]

For the purposes of introducing intense CT character into perylene dyes, it is needed to develop expeditious synthetic pathways toward the perylene dyes with a strong electron-donating character that allows the tuning of the maximium absorption wavelength and oxidation potential, in order to promote excellent electron injection from the dye excited state into the CB of the TiO_2 and to effect charge recombination between the oxidized dye and the I^-/I_3^- redox electolyte.

There are many reports of perylene dyes synthesised for use in DSSCs all of which show diverse structural features due to the regioselective manner that halogenation can be effected onto the perylene core. 1,6,9-Tribromoperylene monoimide (**1**) is conveniently prepared from the commercially available 3,4:9,10-perylene tetracarboxylic dianhydride (**2**) in two well-established synthetic steps.[11, 12] This synthon has enabled access to 1,6,9-trifuctionalized perylene monoanhydrides with

a large degree of structural diversity making it possible to develop efficient photosensitizers. Thus, we chose to investigate the synthesis, characterization and photovoltaic properties of 1,6,9-tris(triarylaminoalkynyl) perylene monoanhydrides **H**, **t-Bu**, and **OMe** (Figure 2).

Figure 2. Structure of the perylenes **H**, **t-Bu**, and **OMe** used in this study.

The convenience of this synthesis is twofold. Firstly, the robustness of the Sonogashira coupling protocol to install alkynyl residues on the perylene ring is fortitous. Then, the nature of the alkynyl-functionalized triarylamine allows the inclusion of electron-donating or sterically-demanding groups by simply utilizing the appropriate, commercially available *N*,*N*-diphenylamine at the beginning of the synthetic pathway.

Results and discussion

Synthesis of materials

The synthesis of the perylene dyes utilized in this study is outlined in Scheme 1. Commercially available 3,4:9,10-perylene tetracarboxylic dianhydride (**2**, PTCDA) was treated with 2,6-diisopropylaniline/$Zn(OAc)_2$ in quinoline/*N*,*N*-dibutylethanolamine at 230°C to afford *N*-(2,6-diisopropylphenyl)-3,4-perylene dicarboximide (**3**).[13] The monoimide was selectively brominated by previously reported procedure to give 1,6,9-tribromo-*N*-(2,6-diisopropylphenyl)perylene-3,4-dicarboximide (**1**)[12, 14, 15] which was to be coupled with terminal alkynes **4**-**6**. In contrast to alkyne **4**,[16] which was synthesized by a previously reported procedure, alkynes **5** and the previously reported **6**[17] were made via Buchwald-Hartwig coupling of the appropriate *para*-substituted diphenylamines to commercially available (4-bromophenylethynyl)trimethylsilane. Subsequent deprotection of the silyl-protecting group with tetra *n*-butylammonium fluoride afforded the required triarylamino-functionalized terminal alkynes in good overall yields. Alkynes **4-6** were utilized in the aforementioned Sonogashira coupling with **1** using previously reported conditions to afford the trialkynylated perylene monoimides (**7-9**) in good yields.[18] Alkaline treatment of the imides (KOH/*t*-BuOH) afforded the target trifunctionalized perylene monoanhydrides **H**, **t-Bu**, and **OMe**.

Scheme 1. Synthesis of perylene dyes **H**, **t-Bu**, and **OMe**. a) 2,6-diisopropylaniline, $Zn(OAc)_2$, quinoline/*N*,*N*-dibutylethanolamine, 230°C, b) Br_2, $CHCl_3$, reflux, c) **4-6,** $Pd(PPh_3)_4$, CuI, THF/ *N*,*N*-diisopropylethylamine (1:1), 80°C 12h, d) KOH, *t*-BuOH, reflux 12h.

Optical properties

The UV-vis absorption spectra of anhydrides **H**, **t-Bu**, and **OMe** in CH_2Cl_2 are given in Figure 3. All of the absorption spectra possess similar features. In particular, the broad absorption at 450-750 nm is noteworthy. This absorption is attributed to a CT absorption of the perylene dye, reslting from the orbital partitioning induced from substitution of a strong donor in the 9-position of the perylene core. Compared to the perylene photosensitizers previously reported by our group,[7] all three dyes in this work displayed improved absorption properties across the visible region of the spectrum due to the presence of the CT absorption. Especially, it is the improvement in the exctinction coefficient that results in improved light-harvesting ability when the dyes are implemented into photovoltaic devices (vide infra). Perylene **H**, exhibits a maximum at its CT absorption, appearing at 574 nm. Within the perylene series presented, it can be seen that *t*-butyl substitution causes a slight red shift in the absorption maximum of **t-Bu**, appearing at 588 nm and demonstrating the ease at which longer wavelength absorption can be achieved through introduction of electron-donating substituents at strategic positions. In a similar manner, perylene **OMe**, possessing the stronger electron-donating methoxy groups, experiences a greater red shift to 595 nm but also a significant increase in exctinction coefficient. This significant increase can be rationalized by the presence of the oxygen atoms whose lone electron pairs increase the size of the π-system within the molecule.

Figure 3. UV-Vis absorption spectra of perylenes **H** (black), **t-Bu** (red), and **OMe** (blue) in CH_2Cl_2.

The fluorescence spectra for compounds **H**, **t-Bu**, and **OMe** in CH_2Cl_2 were obtained by excitation at 573 nm and are presented in Figure 4 The spectra are featureless and of low energy, reminiscent of emission from a CT absorption. The emission maximum of **H** appears at 748 nm. The introduction of the *t*-butyl moiety results in a shift of the emission maximum to 790 nm, whereas inclusion of the methoxy group onto the parent perylene leads to a bathochromic shift to 815 nm. One striking feature of the fluoresence spectra of this series of perylenes is the drastic reduction in the emission intensity recorded upon the inclusion of substituents on the triphenylamine moiety. The reduction in emission intensity can be rationalized by the presence of two deactivation processes upon generation of the excited singlet state of perylene species. One argument is that a greater degree of vibrational relaxation is experienced by perylenes **t-Bu** and **OMe** upon the absorption of light due to the presence six additional *tert*-butyl or methoxy groups, respectively. Due to the presence of these substituents, a reduction in the fluorescence quantum yield can be expected. Secondly, the occurrence of a competing intramolecular electron transfer process can be invoked to rationalize the decrease in emission intensity experienced by the perylene photosensitizers. This phenomenon has been observed in perylene bisimides with electron donating substitutents.[19]

Figure 4. Fluorescence spectra of **H** (black), **t-Bu** (red), and **OMe** (blue) in CH_2Cl_2 (λ_{ex} = 573 nm). The absorbance at 573 nm was adjusted to be identical for comparison.

As perylene dyes **H**, **t-Bu**, and **OMe** are to be used as photosensitizers in DSSCs, estimation of the optical HOMO-LUMO gap is essential in drawing conclusions between the optical/electronic properties of the dye and performace in the corresponding DSSC (vide infra). The data are summarized in Table 1.

Table 1. Absorption/fluorescence maxima and optical bandgaps for **H**, **t-Bu**, and **OMe.**

Dye	λ_{abs} / nm	λ_{em} / nm	$E_{0\text{-}0}$ / eV
H	574	748	1.84
t-Bu	588	790	1.82
OMe	595	815	1.81

Electrochemical properties

The electrochemical properties of the perylene dyes were investigated by using cyclic voltammetry (CV) and diferential pulse voltammetry (DPV). The redox potentials determined by using DPV are summarized in Table 2. The DPV measurements reveal that perylenes **H**, **t-Bu**, and **OMe** possess a reversible first oxidation potential located at +1.23 to 0.96 V vs. NHE, whereas reversible first and second reduction potentials located at –0.53 to -0.58 vs. NHE (Figures S1-3). Integration of the oxidation peak obtained from CV relative to the reduction peak of the perylene moiety (Figure S1-3) reveals that the first oxidation is a three electron process, and is attributed to the oxidation of the electron-donating triarylamine groups.

Figure 5. DPV curves of **H** (black), **t-Bu** (red), **OMe** (blue) (vs. NHE) obtained in CH_2Cl_2 containing 0.1 M Bu_4NPF_6.

An interesting feature that electrochemical analysis revealed is the tunability of the oxidation potential as a function of the substitution on the triarylamino- group. Perylene **H**, possessing no substitution, resulted in E_{ox}= +1.23 V (vs. NHE) whereas Perylene **t-Bu**, functionalized with *t*-butyl groups, possessed E_{ox}= +1.09 V (vs. NHE) and through the inclusion of strongly electron-donating methoxy groups, perylene **OMe** exhibits E_{ox}= +0.96 V (vs. NHE). Thus, by simply changing the substitution on the triarylamino groups, the oxidation potential of the dye can be easily tuned in order to engineer dyes that, upon oxidation, favour fast regeneration by I^-/I_3^- (+0.5 V vs. NHE) in the electrolyte. Moreover, all of the dyes possess excited state potentials more negative than the conduction band of TiO_2 (–0.5 V vs. NHE),[20] making electron injection from the dye into the CB of the TiO_2 thermodynamically possible.

Table 2. Redox potentials as determined by DPV (vs. NHE) obtained in CH_2Cl_2 containing 0.1 M Bu_4NPF_6.

Dye	E_{ox} / V	E_{red} / V	$E_{ox} - E_{red}$ / eV	E_{ox}^* / V
H	+1.23	–0.53	1.76	–0.61
t-Bu	+1.09	–0.58	1.67	–0.73
OMe	+0.96	–0.58	1.54	–0.85

Molecular orbital calculations

To gain further insight into the geometric, electronic and optical properties of perylenes **H**, **t-Bu**, and **OMe** were subjected to *ab initio* calculations, using hybrid density functional theory (DFT) with the 3-21G basis set. The optimized structures of the respective molecules and most importantly, the distribution of frontier orbital thoughout the molecule were calculated and are presented in Figure 6. The calculated energies for the frontier orbitals and the HOMO-LUMO gap (Table 3) are listed in Table 3.

Figure 6. Frontier orbitals of perylenes **H**, **t-Bu**, and **OMe** optimized using B3LYP/3-21G level of theory.

Table 3. Molecular orbital energy levels for perylenes **H**, **t-Bu**, and **OMe**.

Dye	E_{HOMO} / eV	E_{LUMO}/ eV	Bandgap / eV
H	–4.96	–2.95	2.01
t-Bu	–4.82	–2.86	1.96
OMe	–4.68	–2.78	1.90

Two essential features are observed from calulation of the frontier orbitals of the dyes. Firstly, the HOMOs of the perylene dyes are located at the perylene core and the triarylamine substitutents and the LUMOs at the perylene core and the anhydride moiety. Secondly, the trend in the calculated bandgap energy corresponds well with the trends observed by electrochemical and optical measurements (vide supra).

Photovoltaic performance

DSSCs were fabricated using dyes **H**, **t-Bu**, and **OMe** by immersing the TiO_2 electrodes with a double layer structrue of consisting of 12 μm thickness with 20 nm-sized TiO_2 nanoparticles and 4 μm thickness with 400 nm-sized TiO_2 nanoparticles into THF solutions of the perylenes (0.2 mM). Initially, power conversion efficiency (η) was evaluated as a function of immersion time of the electrode in the dye solution. Therefore, immersion times of 1, 3, 6, 12, 24 hours were investigated, the result of which is presented in Figure 7, with an additional immersion time of 48 hours for dye **t-Bu** included in the plot (not shown).

Figure 7. Profiles of η vs. Immersion time for perylenes **H** (black), **t-Bu** (red), and **OMe** (blue)

Perylene **H** shows steady increases in the η as a result of prolonging the immersion time to a maximum of 2.1% after 6 hours. The introduction of *t*-butyl groups in **t-Bu** results in a slow increase in η over prolonged immersion times reaching a maximum of 2.1% at 24 hours immerison. The difference in the optimal immersion time between **H** and **t-Bu** is attributed to lower electron density of the anchoring group in the LUMO of **t-Bu**, causing slower binding of **t-Bu** to the TiO_2 substrate (vide infra). The best performance achieved was for dye **OMe** using an immersion time of 6 hours to yield an η value of 2.9%. However, if the substrate was allowed longer

immersion times than this, a sharp drop in cell performance was observed. To further access the binding behaviour of the dyes as a function of time, amount of dye adsorbed onto the TiO_2 substrate was assessed. This was achieved calculating the amount of dye on dye-adsorbed TiO_2 substrates (1 cm^2). The amount of dye was calculated, assuming no difference between the molar absorption coefficient in solution and on the substrate, and was monitored as a function of immersion time (Figure 8).

The plot in Figure 8 shows that the the 90% saturation for the final adsorbed dye for **H** is achieved after 6 hours immersion time, whereas the sterically demanding **t-Bu** requires at least 24 hours for the majority of the dye to adsorb. This adsorption behaviour parallels the optimal adsorption times for maximum power conversion efficiency for these perylene dyes. However, the case for **OMe** is non-intuitive, in that the dye saturation adsorption is reached at 12 hours, but the corresponding cell experiences a slight decline in the efficiency at and beyond this immersion time. The amounts of dye adsorbed per unit area are rather similar for perylenes **H** and **t-Bu**, are significantly larger than that for **OMe**. The reasoning for this was attributed to a combination of two differences between **H** compared to **t-Bu** and **OMe**. Firstly, the increased molecular size of perylenes **t-Bu** and **OMe** compared to **H** would result in slower binding due to steric limitations during the adsorption process. Secondly, the slight perturbations in the frontier orbitals (as visualized in the *ab initio* calculations in Figure 6) of **t-Bu** and **OMe** located about the anhydride moiety upon introduction of the electron donating substituents to the triphenylamine moieties is suspected to affect the anchoring of the dye. However the observation of **OMe** to achieve a lower power conversion efficiency due to the prolonged immersion time suggests either aggregation of dye on the TiO_2 [20] or an alteration to a more tilted binding geometry of the dye to the TiO_2,[21] both of which have been demonstrated to have profound negative effects on the corresponding cell performance.

Figure 8. Plot of adsorbed dye (mol.cm^{-2}) vs. immersion time (h) for perylenes **H** (black), **t-Bu** (red), and **OMe** (blue).

Figure 9 depicts the photocurrent-voltage characteristics of the TiO_2/dye cells under respective conditions giving maximum performance for each dye (Table 4). Introduction of the *tert*-butyl groups in **t-Bu** results in a slight increase of both the J_{sc} (5.6 mA.cm^{-2}) and the V_{OC} (0.60 V) when compared to the same values for **H** where J_{SC}= 5.0 mA.cm^{-2} and V_{OC}= 0.58 V. Presumably the origins of the larger improvement in photovoltaic parameters in **t-Bu** is a result of reduced electron density of the perylene moiety close to the anchoring group in the HOMO of **t-Bu** achieved by electron-donating alkyl substitution on the triphenylamine donor moieties.[21] The introduction of the stronger electron donating methoxy groups in **OMe** leads to the further increase of both the V_{OC} (V_{OC}= 0.61 V) and J_{SC} (J_{SC}= 6.5 mA.cm^{-2}). This can be correlated well to the further decrease in electron density of the perylene moiety close to the anchoring group in the HOMO of **OMe** achieved by more electron-donating alkoxy substitution on the triphenylamine donor moieties as well as improved light-harvesting property due to the larger molar absorption coefficient of **OMe**.[21]

Figure 9. Photocurrent-voltage characteristics of perylenes **H** (black), **t-Bu** (red), and **OMe** (blue). Conditions: electrolyte 0.1 M LiI, 0.05 M I_2, 0.6 M 2,3-dimethyl-1-propyl imidazolium iodide and 0.5 M 4-*t*-butylpyridine in CH_3CN; input power AM 1.5 under simulated solar light 100 mW cm^{-2})

Table 4. Photovoltaic data under optimised conditions.

Dye	J_{SC} / mA.cm^{-2}	V_{OC} / V	*ff*	η/ %	Immersion time (h)
H	5.0	0.58	0.74	2.1	6
t-Bu	5.6	0.60	0.74	2.1	24
OMe	6.5	0.61	0.72	2.9	6

Photocurrent action spectra were obtained on the optimized cells and they follow the absorption features of the corresponding perylenes adsorbed on the electrode, indicating that the perylene dye is responsible for photocurrent generation. Perylenes **H** and **t-Bu** displayed IPCE spectra of comaprable breadth but the maximum IPCE of **t-Bu** (42% at 510 nm) eclipsed that of **H** (34% at 510 nm). Perylene **OMe** recorded the highest IPCE value (43% at 505 nm) as well as the broadest IPCE spectrum, with the absorption ceasing at ~700 nm. The presence of the electron donating groups on **t-Bu** and **OMe** contributed positively to the improvement of the higher IPCE in the corresponding devices, compared to **H**. This matches the trend that the driving force increases with introducing more electron-donating groups into the amine moieties (Table 2), leading to more efficient electron injection from the perylene excited singlet state to the CB of the TiO_2.[23] Furthermore, it demonstrates how the favourable tuning of dye properties (λ_{max} and E_{ox}) enables **OMe** to overcome the intense quenching of fluorescence (as observed by steady-state fluoresence spectra) to undergo efficient electron injection into the TiO_2 substrate, resulting in improved light harvesting ability. Thus, both tuning E_{ox} as well as extension of the π-electron system facilitated favourable electron injection and longer wavelength absorption maximum observed in the IPCE spectrum respectively, resulting in the higher efficiency observed by this device.

Figure 10. IPCE spectra of perylenes **H** (black), **t-Bu** (red), and **OMe** (blue).

Experimental

General

All chemicals were of reagent grade quality, purchased and used without further purification. Solvents were purchased

from Wako Chemicals (Japan) and used as received. Anhydrous THF was distilled from a benzophenone ketyl/sodium still. Column chromatography and thin-layer chromatography (TLC) were performed with UltraPure Silica Gel (230-400 mesh, SiliCycle) and Silica gel 60 F_{254} (Merck), respectively. ^{1}H NMR specra were acquired on a JEOL EX-400 (400 MHz) or a JEOL AL-300 (300 MHz) spectrometer. UV-vis absorption spectra were measured using a Perkin-Elmer Lambda 900 UV/VIS/NIR Spectrophotometer. Fluorescence FT-IR Spectra were recorded on a JASCO FT/IR-470 plus spectrometer, using a KBr pellet. High-resolution mass spectra were acquired using FAB and EI. Elemental analyses were performed at Kyoto University. Electrochemistry was performed on an ALS 630a electrochmical analyzer using CH_2Cl_2 containing 0.1M tetrbutylammonium hexafluorophosphate (Bu_4NPF_6) as the supporting electrolyte. A glassy carbon electrode (3 mm diameter), $Ag/AgNO_3$ (0.01 M in CH_3CN) and a Pt wire counterelectrode were used in all cases. Ferrocene/ferrocenium (Fc/Fc^+, +0.642 V vs. NHE) or decamethylferrocene ($Me_{10}Cp/Me_{10}Cp^+$, +0.076 V vs. NHE) were used as the internal reference for the samples to enable conversion of obtained values to the NHE scale. DFT calculations were performed using Gaussian 03 and orbitals were visualized using the Molstudio 3.0 package.

Dye Sensitized Solar Cells

UV-vis absorption measurements of the perylenes adsorbed on TiO_2 were performed using TiO_2 (20 nm) with a thickness of 12 µm without a light scattering layer.

Preparation of TiO_2 electrodes and the fabrication of sealed DSSCs were performed using the previously reported literature method.[24,25] Nanocrystalline TiO_2 paste (20 nm CCIC:PST18NR, JGC-CCIC) was used as the transparent semiconducting substrate on the photoanode for dye adsorption and submicrocrystalline TiO_2 (400 nm particles, CCIC:PST400C, JGC-CCIC) was used to provide a light scattering layer. The working electrode was prepared by cleaning FTO glass (Solar, 4 mm thick, 10 Ω/Sheet, Nippon Sheet Glass) with a detergent solution (distilled water) in an ultrasonic bath for 10 minutes, rinsing with distilled water, ethanol and air drying. The electrode was subjected to UV-O_3 irradiation (18 min), immersion into a solution of freshly prepared 40 mM $TiCl_{4(aq)}$ at 70°C for 30 min, washing with distilled water, ethanol and air drying. Nanocrystalline TiO_2 was coated onto the FTO by screen printing (area 0.25 cm^2, 5 mm × 5 mm), folowed by standing in a clean box for a few minutes and dried at 125°C for 6 min, repeating to attain a final thickness of 12 µm. The thickness of the films was determined using a surface profiler (SURFCOM 130A, ACCRETECH) A layer of 4 µm submicrocrystalline TiO_2 paste was deposited in the same fashion as the nanocrystalline layer. The electrode was heated under an airflow at 325°C for 5 min, 375°C for 5 min, 450°C for 15 min and 500°C for 15 min. The electrode was then subjected to immersion into 40mM $TiCl_{4(aq)}$ at 70°C for 30 min before rinsing with distilled water and ethanol and air drying. Prior to immersion into dye solutions, the electrodes were scintered at 500°C, cooled to 70°C and immersed into the dye solution and incubated at 25°C in the dark for the prescribed times.

The counter electrode was prepared by drilling a small hole in FTO glass (Solar, 1 mm thick, 10 Ω/Sheet, Nippon Sheet Glass), rinsing with distilled water and ethanol before treatment with 0.1 M HCl/2-propanol in a ultrasonic bath for 5 minutes (removal of iron contamintion). Counter electrodes were washed with water and ethanol followed by ultrasonication in acetone and heating in air at 400°C for 15 min. Platinum was deposited by coating the electrode with a solution of H_2PtCl_6 (2 mg in 1 mL EtOH) twice and heating in air at 400°C for 15 minutes.

The sandwich cell was prepared by assembling the photoanode and the counter electrode together, using a hotmelt-ionomer film (Surlyn, DuPont) at 130°C. Surlyn was also used to cover the hole drilled on the back of the counter electrode, to allow vacuum backfilling of the cell with the electrolyte. The drilled hole was finally covered with another piece of surlyn film and a cover glass (0.13-0.17 mm thick). The exposed FTO on the cell was roughened with sandpaper to allow the application of solder to the edge of the FTO electrodes. The electrolyte used was composed of 0.1 M LiI, 0.05 M I_2, 0.6 M 2,3-dimethyl-1-propyl imadazolium iodide and 0.5 M 4-*tert*-butylpyridine in CH_3CN.

Photocurrent action spectra were obtained using the PEC-S20 (Peccell Technologies) action spectrum meaurement apparatus. Photocurrent-voltage (*I-V*) characteristics were measured using a solar simulator (PEC-L10, Peccell Technologies) with simulated sunlight of AM 1.5 (100 mW cm^{-2}) using a mask of black plastic tape to limit the amount of scattering light to TiO_2 film area.

Synthesis

All chemicals were purchased and used without purification. Synthesis of *N*-(2,6-diisopropylphenyl)-3,4-perylene dicarboximide (**3**)[13] 1,6,9-tribromo-*N*-(2,6-diisopropylphenyl)perylene-3,4-dicarboximide (**1**)[12], 4-ethynyltriphenylamine (**4**)[16] were prepared as per literature methods.

Synthetic Methods

Bis(4-*tert*-butylphenyl)aminephenylacetylene-TMS protected (5-TMS).

Bis(4-*tert*-butylphenyl)amine (1.01 g, 3.59 mmol), (4-bromophenylethynyl)trimethylsilane (1.00 g, 3.95 mmol), NaOBu-*t* (431 mg, 4.48 mmol), $Pd_2(dba)_3$ (33 mg, 0.0359 mmol,), P(*t*-Bu)$_3$ (10% in hexane, 0.0592 mmol, 120 µL) in toluene (25 mL) was degassed for 10 minutes with Ar then heated at 80°C for 12 hours. The solvent was evaporated and the residue subjected to column chromatography on silica using CH_2Cl_2 to give the desired product as a white solid (1.24 g, 72%); m.p. 134-136°C; δ_H(300 MHz; CD_2Cl_2) 1.31 (18 H, s, 2 × t-Bu), 6.91 (2 H, d, Ar-*H*, *J* 6.6), 7.00 (4 H, d, 2 × Ar-*H*, *J* 6.3), 7.25 (4 H, d, 2 × Ar-*H*, *J* 6.3), 7.27 (2H, d, *J* 6.6, Ar-*H*); δ_C(75 MHz; CD_2Cl_2) -0.2, 31.4, 34.5, 92.7, 105.8, 114.9, 120.9, 125.1, 126.5, 132.9, 144.6, 147.1, 148.8; IR

(KBr cell): ν_{max}/cm^{-1} 3035 (Ar-H), 2960 (CH_3), 2902, 2867 (Ar-H) 2154 (Alkyne C-C), 1598, 1503 (Ar-H), 1322, 1282 (C-N), 1249 (Si-CH_3), 865, 840 (*para*-substituted Ar); *m/z* (EI) 453.2849 (M^+. $C_{31}H_{39}NSi$ requires 453.2852).

Bis(4-*tert*-butylphenyl)aminephenylacetylene (5).

5-TMS (1.24 g, 2.57 mmol) in CH_2Cl_2 (15 mL) was cooled to 0°C and TBAF (1M in THF, 3.75 mmol, 3.75 mL) was added in a dropwise manner. The resulting solution stirred at 0°C for 1 hour then at room temperature overnight. The solvents were evaporated and the residue purified by column chromatography on silica eluting with CH_2Cl_2 to give **5** as a white solid (922 mg, 94%); m.p. 138-140°C; δ_H(300 MHz; CD_2Cl_2) 1.31 (18 H, s, 2 × Ar-C(C*H*$_3$)$_3$), 6.89 (2 H, d, Ar-*H*, *J* 8.7), 7.01 (4 H, d, 2 × Ar-*H*, *J* 8.7), 7.28 (2 H, d, Ar-*H*, *J* 8.7), 7.31 (4 H, d, 2 × Ar-*H*, *J* 8.7); δ_C(75 MHz; CD_2Cl_2) 31.5, 34.6, 76.1, 84.4, 113.8, 121.0, 125.3, 126.7, 133.2, 144.7, 147.3, 149.2; IR (KBr cell): ν_{max}/cm^{-1} 3295 (Alkyne C-H), 3037 (Ar-H), 2961 (CH_3), 2901, 2866 (Ar-H), 2104 (Alkyne C-C), 1598, 1504 (Ar-H), 1322, 1284 (C-N), 831 (*para*-substituted Ar); *m/z* (EI) 381.2464 (M^+. $C_{20}H_{31}N$ requires 381.2457).

Bis(4-methoxyphenyl)aminephenylacetylene-TMS protected (6-TMS).

Bis(4-methoxyphenyl)amine (500 mg, 2.18 mmol) (4-bromophenylethynyl)trimethylsilane (610 mg, 2.4 mmol) NaOBu-*t* (262 mg , 2.73 mmol) $Pd_2(dba)_3$ (20mg, 0.022mmol) P(*t*-Bu)$_3$ (10% solution in hexane, 66 µL, 0.033mmol) in toluene (13 mL) was degassed with argon for 10 minutes) then heated at 80°C for 12 hours. The solvents were evaporated and the residue subjected to column chromatography on silica using hexane/$CHCl_3$ (1:3) as the eluant to give **6-TMS** as a yellow solid (660 mg, 75%); δ_H(400 MHz; CD_2Cl_2) 0.24 (9 H, s, Si(C*H*$_3$)$_3$), 3.78 (6 H, s, 2 × Ar-OC*H*$_3$), 6.77 (2 H, d, Ar-*H*, *J* 8.8), 6.86 (4 H, d, 2 × Ar-*H*, *J* 8.8), 7.06 (4 H, d, 2 × Ar-*H*, *J* 8.8), 7.23 (2 H, d, Ar-*H*, *J* 8.8); δ_C(100 MHz; CD_2Cl_2) -0.2, 55.6, 92.3, 106.0, 113.7, 115.0, 118.7, 127.5, 132.8, 140.2, 149.3, 156.8; *m/z* (EI) 401.1815 (M^+. $C_{25}H_{27}NO_2Si$ requires 401.1811).

Bis(4-methoxyphenyl)aminephenylacetylene (6).

6-TMS (555 mg, 1.38 mmol) in CH_2Cl_2 was cooled to 0°C and TBAF (1M in THF, 2.67 mmol, 2.67 mL) was added dropwise. The solution was stirred for 2 hours at 0°C and the solvents evaporated. The residue was subjected to column chromatography on silica eluting with CH_2Cl_2 to give **6** as a yellow solid (432 mg, 95%); δ_H(400 MHz; CD_2Cl_2) 3.01 (1 H, s, ArCC-*H*), 3.76 (6 H, s, 2 × Ar-OC*H*$_3$), 6.76 (2 H, d, Ar-*H*, *J* 8.8), 6.83 (4 H, d, 2 × Ar-*H*, *J* 8.8), 7.05 (4 H, d, 2 × Ar-*H*, *J* 8.8), 7.23 (2 H, d, Ar-*H*, *J* 8.8); δ_C(100 MHz; CD_2Cl_2) 55.8, 75.8, 84.5, 112.6, 115.2, 118.9, 127.7, 133.2, 140.3, 149.7, 156.9; *m/z* (EI) 329.1414 (M^+. $C_{22}H_{19}NO_2$ requires 329.1416).

Triphenylamine perylene imide (7).

1 (200 mg, 0.279 mmol), CuI (27 mg, 0.15 mmol), $Pd(PPh_3)_4$ (32 mg, 0.028 mol) in THF (10 mL) and *N*,*N*-Diisopropylethylamine (10 mL) was degassed with Ar for 30 mins. **4** (245 mg, 0.91 mmol) was added and the mixture stirred for 15 hours at 80°C. The reaction mixture was diluted with HCl (2N, 80 mL), extracted with CH_2Cl_2 (2 × 50 mL), the organics dried ($MgSO_4$) and evaporated. The dark solid was purified by column chromatography on silica, eluting with $CHCl_3$/Hexane (2:1) to remove the starting material then $CHCl_3$ to elute **7** as a black solid (308 mg, 85%); m.p. >300°C; δ_H(400 MHz; CD_2Cl_2) 1.16 (12 H, d, 2 × CH(C*H*$_3$)$_2$, *J* 6.8), 2.78 (2 H, quintet, 2 × C*H*(CH$_3$)$_2$, *J* 6.8), 7.02 (2 H, d, Ar-*H*, *J* 8.8), 7.03 (2 H, d, Ar-*H*, *J* 8.8), 7.04 (2 H, d, Ar-*H*, *J* 8.8), 7.08-7.15 (18 H, m, Ar-*H*), 7.28-7.36 (16 H, m, Ar-*H*), 7.48 (4 H, 2 × d, 2 × Ar-*H*, *J* 8.8), 7.52 (2 H, d, Ar-*H*, *J* 8.8), 7.79 (1 H, t, Pery-*H*, *J* 8.3), 7.88 (1 H, d, Pery-*H*, *J* 8.3), 8.60 (1 H, d, Pery-*H*, *J* 8.3), 8.79 (1 H, s, Pery-*H*), 8.80 (1 H, s, Pery-*H*), 9.84 (1 H, d, Pery-*H*, *J* 8.3), 9.96 (1 H, d, Pery-*H*, *J* 8.3); δ_C(100 MHz; CD_2Cl_2) 24.2, 29.6, 87.5, 91.2, 91.3, 96.8, 97.1, 99.1, 115.2, 115.3, 115.4, 118.9 (2 × s), 120.4 (2 × s), 121.9 (2 × s), 122.0, 124.4, 124.5, 124.9, 125.8, 125.9, 126.9, 127.8, 128.0, 128.3, 128.8 (2 × s), 129.0, 129.2, 129.9 (3 × s), 130.2, 131.7, 133.1, 133.2, 133.2 (2 × s), 136.6, 137.0, 138.1, 138.2, 146.5, 147.3, 147.4, 149.1, 149.2 (2 × s), 163.9 (2 × s); IR (KBr cell): ν_{max}/cm^{-1} 3035 (Ar-H), 2861 (Ar-H), 2184 (Alkyne C-C), 1705, 1667 (Imide C-O), 1590, 1506 (Ar-H), 1313, 1280 (C-N), 753, 695 (Ar-H); *m/z* (FAB) 1282.5211 (M^+. $C_{94}H_{66}N_4O_2$ requires 1282.5186).

Triphenylamine perylene anhydride (H).

7 (310 mg, 0.276 mmol), KOH (1.5 g, 27.6 mmol) and *t*-BuOH (70 mL) were combined and the mixture heated at reflux for 3 hours. Upon cooling to room temperature, HCl (2N, 250 mL) was added and the mixture stirred overnight. The organics were extracted with CH_2Cl_2 (3 × 50 mL), dried ($MgSO_4$) and the solvent evaporated. The black solid was purified by column chromatography on silica eluting with $CHCl_3$. Precipitation of the product from CH_2Cl_2/MeOH washing with MeOH and drying on high vacuum afforded **H** as a black solid (223 mg, 72%); m.p. >300°C; (Found C, 87.2; H, 4.6; N, 3.7; $C_{82}H_{49}N_3O_3$ requires C, 87.6 ; H, 4.4 ; N, 3.7 %); δ_H(400 MHz; CD_2Cl_2) 6.90 (2 H, d, Ar-*H*, *J* 8.8), 6.93 (2 H, d, Ar-*H*, *J* 8.3), 6.94 (2 H, d, Ar-*H*, *J* 8.8), 7.04-7.12 (20 H, m, Ar-*H*), 7.18 (1 H, d, Pery-*H*, J 8.3) 7.25-7.36 (16 H, m, Ar-*H*), 7.38 (1 H, t, Pery-*H*, *J* 8.3), 8.06 (1 H, s, Pery-*H*), 8.13 (1 H, s, Pery-*H*), 8.15 (1 H, d, Pery-*H*, *J* 8.3), 9.26 (1 H, d, Pery-*H*, *J* 8.3), 9.46 (1 H, d, Pery-*H*, *J* 8.3); δ_C(100 MHz; CD_2Cl_2) 77.9, 87.3, 90.7, 90.8, 98.6, 98.9, 99.5, 114.6, 114.7, 114.8 (2 × s), 115.4, 117.6, 117.7, 121.5, 121.6, 121.7, 124.4 (2 × s), 125.0, 125.8, 125.9, 126.7, 126.9, 127.3, 127.4, 127.6, 127.9, 128.2, 129.4, 129.6, 129.9, 132.1, 132.7, 132.9, 133.1, 135.3, 135.9, 138.9, 139.1, 147.2, 147.3, 147.4, 148.9, 149.1, 159.4; IR (KBr cell): ν_{max}/cm^{-1} 3035 (Ar-H), 2923, 2852 (Ar-H), 2183 (Alkyne C-C), 1769, 134 (Anhydride C-O), 1587, 1507 (Ar-H), 1268 (C-N), 753, 694 (Ar-H); *m/z* (FAB) 1123.3762 (M^+. $C_{82}H_{49}N_3O_3$ requires 1123.3774).

4-*tert*-butyltriphenylamine perylene imide (8).

1 (200 mg, 0.279 mmol) CuI (27 mg,) $Pd(PPh_3)_4$ (38 mg,) in THF (10 mL) and *N*,*N*-diisopropylethylamine (10 mL) was degassed with Ar for 20 mins. **5** (401 mg, 1.05 mmol) was added and the mixture stirred for 15 hours at 80°C. The

reaction mixture was diluted with HCl (2N, 80 mL), extracted with CH_2Cl_2 (3 × 50 mL), the organics dried ($MgSO_4$) and evaporated. The dark solid was purified by column chromatography on silica, eluting with $CHCl_3$/Hexane (2:1) to remove the starting material then $CHCl_3$ to elute **8** as a black solid (346 mg, 77%); m.p. >300°C; δ_H(400 MHz; CD_2Cl_2) 1.14 (12 H, d, 2 × CH(CH_3)$_2$, *J* 6.8), 1.32 (36 H, s, 2 × C(CH_3)$_3$), 1.33 (18 H, s, C(CH_3)$_3$), 2.76 (2 H, quintet, 2 × CH C*H*(CH_3)$_2$, *J* 6.8), 6.97-7.00 (6 H, m, Ar-*H*), 7.08 (12 H, d, Ar-*H*, *J* 8.5), 7.28-7.35 (14 H, m, Ar-*H*), 7.45-7.52 (7 H, m, Ar-*H*), 7.84 (1 H, t, Pery-*H*, *J* 8.0), 7.93 (1 H, d, Pery-*H*, *J* 8.0), 8.65 (1 H, d, Pery-*H*, *J* 8.0), 8.82 (1 H, s, Pery-*H*), 8.84 (1 H, s, Pery-*H*), 9.93 (1 H, d, Pery-*H*, *J* 8.0), 10.02 (1 H, d, Pery-*H*, *J* 8.0); δ_C(75 MHz; CD_2Cl_2) 31.6, 34.7, 87.4, 91.1, 97.1, 97.3, 99.4, 114.2 (2 × s), 114.4, 119.0, 120.3 (2 × s), 120.7, 120.9, 124.5, 125.1, 125.5, 125.6, 126.8, 127.8, 127.9, 128.0, 128.7, 129.0, 129.2, 129.2, 129.8, 129.9, 130.1, 131.7, 132.9, 133.0, 133.2, 135.6, 136.5, 136.8, 138.0, 138.1, 144.5, 144.6, 146.5, 147.6, 147.6, 149.4, 149.5, 149.6, 163.9; IR (KBr cell): ν_{max}/cm^{-1} 3035 (Ar-H), 2961 (CH_3), 2868 (Ar-H), 2186 (Alkyne C-C), 1709, 1670 (Imide C-O), 1597, 1507 (Ar-H), 1320, 1297 (C-N), 829 (*para*-substituted Ar); *m/z* (FAB) 1618.8905 (M^+. $C_{118}H_{114}N_4O_2$ requires 1618.8942).

4-*tert*-butyltriphenylamine perylene anhydride (t-Bu).
8 (300 mg, 0.234 mmol) and KOH (1.32 g, 23.4 mmol) in *t*-BuOH (70 mL) was heater at reflux for 4 hours. The reaction mixture was cooled to room temperature and poured into HCl (2N, 240 mL). the organics were extracted with DCM (3 × 50mL), the organics dried ($MgSO_4$) and evaporated. The dark solid was subjected to column chromatography on silica eluting with $CHCl_3$ and precipitated from $CHCl_3$/MeOH to afford **t-Bu** as a black solid. (208 mg , 61%); m.p. >300°C; (Found C, 87.7; H, 6.7; N, 2.9; $C_{106}H_{97}N_3O_3$ requires C, 87.2 ; H, 6.7 ; N, 2.9 %); δ_H(400 MHz; CD_2Cl_2) 1.31 (18 H, s, C(CH_3)$_3$), 1.32 (18 H, s, C(CH_3)$_3$), 1.33 (18 H, s, C(CH_3)$_3$), 6.80 (2 H, d, Ar-*H*, *J* 8.8), 6.84 (2 H, d, Ar-*H*, *J* 8.8), 6.88 (2 H, d, Ar-*H*, *J* 8.8), 7.00-7.07 (14 H, m, Ar-*H*), 7.13-7.20 (4 H, m, Ar-*H* and Pery-*H*), 7.27-7.31 (14 H, m, Ar-*H*), 7.92 (1 H, s, Pery-*H*), 7.97 (1 H, d, Pery-*H*, *J* 8.0), 8.00 (1 H, s, Pery-*H*), 9.11 (1 H, d, Pery-*H*, *J* 8.0), 9.31 (1 H, d, Pery-*H*, *J* 8.0); δ_C(100 MHz; CD_2Cl_2) 31.6, 31.7, 34.7, 87.2, 90.7, 90.8, 98.9, 99.0, 113.9, 114.0, 114.5, 115.0, 115.1, 118.1, 118.2, 120.6, 120.7, 120.9, 125.2, 125.5, 125.6, 126.2, 126.8, 127.1, 127.2, 127.7, 127.9 (2 × s), 128.2, 128.4, 129.5, 130.0, 132.3, 132.8, 132.9, 133.1, 135.8, 136.3, 139.0, 139.2, 144.5 (2 × s), 144.6, 147.3, 147.4, 149.2, 149.4, 159.7; IR (KBr cell): ν_{max}/cm^{-1} 3035 (Ar-H), 2960 (CH_3), 2902, 2867 (Ar-H), 2185 (Alkyne C-C), 1770, 1740 (Imide C-O), 1597, 1506 (Ar-H), 1322, 1268 (C-N), 829 (*para*-substituted Ar); *m/z* (FAB) 1459.7513 (M^+. $C_{106}H_{97}N_3O_3$ requires 1459.7530).

4-Methoxytriphenylamine perylene imide (9).
1 (137 mg, 0.191 mmol) CuI (18 mg, 0.095 mmol) $Pd(PPh_3)_4$ (22 mg, 0.019 mmol) in THF (6.9 mL) and *N*,*N*-Diisopropylethylamine (6.9 mL) was degassed with Ar for 10 mins. **6** (233 mg, 0.707 mmol) was added and the mixture stirred for 15 hours at 80°C. The reaction mixture was diluted with HCl (2N, 100 mL), extracted with CH_2Cl_2 (3 × 50 mL), the organics dried ($MgSO_4$) and evaporated. The dark solid was purified by column chromatography on silica, eluting with $CHCl_3$/Hexane (2:1) to remove the starting material then $CHCl_3$ to elute **9** as a black solid (255 mg, 91%); m.p. >300°C; δ_H(400 MHz; CD_2Cl_2) 1.15 (12 H, d, CH(CH_3)$_2$, *J* 6.8), 2.77 (2 H, quintet, 2 × CH C*H*(CH_3)$_2$, *J* 6.8), 3.78 (12 H, s, 2 × -OCH_3), 3.79 (6 H, s, -OCH_3), 6.82- 6.89 (18 H, m, Ar-*H*), 7.10 (12 H, d, Ar-*H*, *J* 8.0), 7.33-7.40 (6 H, m, Ar-*H*), 7.43 (2 H, d, Ar-*H*, *J* 8.0), 7.49 (1 H, t, Ar-*H*, *J* 8.0), 7.75 (1 H, t, Pery-*H*, *J* 8.0), 7.83 (1 H, d, Pery-*H*, *J* 8.0), 8.58 (1 H, d, Pery-*H*, *J* 8.0), 8.75 (1 H, s, Pery-*H*), 8.76 (1 H, s, Pery-*H*), 9.83 (1H, d, Pery-*H*, *J* 8.0), 9.95 (1 H, d, Pery-*H*, *J* 8.0); δ_C(100 MHz; CD_2Cl_2) 24.1, 29.6, 55.8, 77.9, 87.2, 91.0, 97.4, 97.6, 99.6, 113.1 (2 × s), 113.3, 115.3, 118.8 (2 × s), 118.9, 119.0, 119.1, 120.2, 120.3, 124.4, 125.1, 126.7, 127.7, 127.8, 127.9 (2 × s), 128.6, 128.0, 129.2, 129.3, 129.8, 129.9, 130.0, 131.7, 132.9, 133.0, 133.2, 136.4, 136.7, 137.9, 138.0, 140.1, 140.2, 146.5, 149.9, 150.1 (2 × s), 157.2 (2 × s), 163.9; IR (KBr cell): ν_{max}/cm^{-1} 3038 (Ar-H), 2996, 2959 (CH_3), 2923 2903, 2832 (Ar-H), 2184 (Alkyne C-C), 1705, 1667 (Imide C-O), 1599, 1504 (Ar-H), 1242 (C-N), 827 (*para*-substituted Ar); *m/z* (FAB) 1462.5859 (M^+. $C_{100}H_{78}N_4O_8$ requires 1462.5820).

4-Methoxytriphenylamine perylene anhydride (OMe).
9 (167 mg, 0.114 mmol) and KOH (640 mg, 11.4 mmol) in *t*-BuOH (35 mL) was heated at reflux for 8 hours. The reaction mixture was cooled and poured into HCl (2N, 240 mL) the mixture was extracted with CH_2Cl_2 (3 × 50 mL), dried ($MgSO_4$) and evaporated. The remaining solids were purified by column chromatography on silica $CHCl_3$ and precipitated from $CHCl_3$/MeOH to afford **OMe** as a black solid (74 mg, 50%); m.p. >300°C; (Found C, 79.8; H, 4.9; N, 3.2; $C_{88}H_{61}N_3O_9$ requires C, 81.0 ; H, 4.7 ; N, 3.2 %); δ_H(400 MHz; CD_2Cl_2) 3.78 (6 H, s, O-CH_3), 3.79 (6 H, s, O-CH_3), 3.80 (6 H, s, O-CH_3), 6.74 (2 H, d, Ar-*H*, *J* 8.8), 6.77 (2 H, d, Ar-*H*, *J* 8.8), 6.81 (2 H, d, Ar-*H*, *J* 8.8), 6.82-6.88 (12 H, m, Ar-*H*), 7.03-7.10 (14 H, m, Ar-*H* and Pery-*H*), 7.17 (2 H, d, Ar-*H*, *J* 8.8), 7.26 (2 H, d, Ar-*H*, *J* 8.8), 7.31 (2 H, d, Ar-*H*, *J* 8.8), 8.03 (1 H, s, Pery-*H*), 8.08 (1 H, d, Pery-*H*, *J* 8.0), 8.09 (1 H, s, Pery-*H*), 9.24 (1 H, d, Pery-*H*, *J* 8.0), 9.44 (1 H, d, Pery-*H*, *J* 8.0); δ_C(100 MHz; CD_2Cl_2) 55.9, 87.1, 90.7, 98.9, 99.1, 99.9, 125.1, 126.2, 127.1 (2 × s), 127.3, 127.8, 127.9, 128.2, 128.4, 128.8, 129.4, 130.0, 132.4, 132.8, 132.9, 133.2, 135. 8, 136.3, 139.0, 139.1, 140.1 (2 × s), 140.2, 149.7, 149.8 (2 × s), 149.9, 157.1 (2 × s), 159.9; IR (KBr cell): ν_{max}/cm^{-1} 3037 (Ar-H), 2995, 2948 (CH_3), 2929, 2903, 2832 (Ar-H), 2183 (Alkyne C-C), 1766, 1734 (Anhydride C-O), 1599, 1503 (Ar-H), 1241 (C-N), 826 (*para*-substituted Ar); *m/z* (FAB) 1303.4447 (M^+. $C_{100}H_{78}N_4O_8$ requires 1303.4408).

Conclusions

We have successfully prepared novel perylene dyes bearing strong electron-donating, three-triarylamine groups for the first time. With introducing more electron-donating group into the three-triarylamine moieties the device performance was

improved considerably. The improvement can be explained by the distribution of the electron density in the HOMO of the perylene moiety, the electron injection effciency, and the light-harvesting property of the perylene dyes. Such fundamental information will be useful for the molecular design of novel dyes exhibiting high device performance.

Acknowledgements

S.M is grateful to the Japanese Society for the Promotion of Science (JSPS) for a JSPS Postdoctoral Fellowship for Foreign Researchers

References

[a] *Institute for Integrated Cell-Material Sciences (iCeMS), Kyoto University, Nishikyo-ku, Kyoto 615-8510, Japan.*
[b] *Department of Molecular Engineering, Graduate School of Engineering, Kyoto University, Nishikyo-ku, Kyoto 615-8510, Japan.*
[c] *Fukui Institute for Fundamental Chemistry, Kyoto University, Sakyo-ku, Kyoto 606-8103, Japan. Fax: +81 75 383 2571; Tel: +81 75 383 2566; E-mail: Imahori@scl.kyoto-u.ac.jp*

† Electronic Supplementary Information (ESI) available: [voltammetric data and ^{1}H and ^{13}C NMR data for **H**, **t-Bu**, and **OMe**]. See DOI: 10.1039/b000000x/

1. B. O'Regan and M. Grätzel, *Nature*, 1991, **353**, 737-740.
2. R. Jose, V. Thavasi and S. Ramakrishna, *J. Am. Ceramic Soc.*, 2009, **92**, 289-301.
3. F. Odobel, L. Le Pleux, Y. Pellegrin and E. Blart, *Acc. Chem. Res.*, 2010, **43**, 1063-1071.
4. C.Y. Chen, M. Wang, J.Y. Li, N. Pootrakulchote, L. Alibabaei, C.h. Ngoc-le, J.D. Decoppet, J.H. Tsai, C. Grätzel, C.G. Wu, S.M. Zakeeruddin and M. Grätzel, *ACS Nano*, 2009, **3**, 3103-3109.
5. H. Imahori, T. Umeyama and S. Ito, *Acc. Chem. Res.*, 2009, **42**, 1809-1818.
6. W. Herbst, *Industrial Organic Pigments: Production, Properties, Applications*, 2003.
7. Y. Shibano, T. Umeyama, Y. Matano and H. Imahori, *Org. Lett.*, 2007, **9**, 1971-1974.
8. T. Edvinsson, C. Li, N. Pschirer, J. Schöneboom, F. Eickemeyer, R. d. Sens, G. Boschloo, A. Herrmann, K. Müllen and A. Hagfeldt, *J. Phys. Chem. C.*, 2007, **111**, 15137-15140.
9. C. Li, J.H. Yum, S.J. Moon, A. Herrmann, F. Eickemeyer, N. G. Pschirer, P. Erk, J. Schöneboom, K. Müllen, M. Grätzel and M. K. Nazeeruddin, *ChemSusChem*, 2008, **1**, 615-618.
10. C. Li, J. Schöneboom, Z. Liu, N. G. Pschirer, P. Erk, A. Herrmann and K. Müllen, *Chem. Eur. J.*, 2009, **15**, 878-884.
11. U. Rohr, C. Kohl, K. Müllen, A. van de Craats and J. Warman, *J. Mat. Chem.*, 2001, **11**, 1789-1799.
12. K. Tomizaki, P. Thamyongkit, R. S. Loewe and J. S. Lindsey, *Tetrahedron*, 2003, **59**, 1191-1207.
13. M. Koenemann, P. Blaschka and H. Reichelt, *Ger. Pat.*, DE102004054303, 2006.
14. H. Quante and K. Müllen, *Angew. Chem. Int. Ed. Engl.*, 1995, **34**, 1323-1325.
15. D. Gosztola, M. P. Niemczyk and M. R. Wasielewski, *J. Am. Chem. Soc.*, 1998, **120**, 5118-5119.
16. S. P. McIlroy, E. Cló, L. Nikolajsen, P. K. Frederiksen, C. B. Nielsen, K. V. Mikkelsen, K. V. Gothelf and P. R. Ogilby, *J. Org. Chem.*, 2005, **70**, 1134-1146.
17. J.H. Lin, A. Elangovan and T.I. Ho, *J. Org. Chem.*, 2005, **70**, 7397-7407.
18. Z. An, S. A. Odom, R. F. Kelley, C. Huang, X. Zhang, S. Barlow, L. A. Padilha, J. Fu, S. Webster, D. J. Hagan, E. W. Van Stryland, M. R. Wasielewski and S. R. Marder, *J. Phys.Chem. A.*, 2009, **113**, 5585-5593.
19. J. Huang, Y. Wu, H. Fu, X. Zhan, J. Yao, S. Barlow, S. R. Marder, *J. Phys. Chem. A.*, 2009, **113**, 5039-5046.
20. H. Imahori, S. Hayashi, H. Hayashi, A. Oguro, S. Eu, T. Umeyama and Y. Matano, *J. Phys. Chem. C.*, 2009, **113**, 18406-18413.
21. H. Imahori, S. Kang, H. Hayashi, M. Haruta, H. Kurata, S. Isoda, S. E. Canton, Y. Infahsaeng, A. Kathiravan, T. Pascher, P. Chábera, A. P. Yartsev and V. Sundström, *J. Phys.Chem. A.*, 2010, DOI: 10.1021/jp103747t.
22. J. N. Clifford, E. Palomares, M. K. Nazeeruddin, M. Grätzel, J. Nelson, X. Li, N. J. Long and J. R. Durrant, *J. Am. Chem. Soc.*, 2004, **126**, 5225-5233.
23. K. Hara, T. Sato, R. Katoh, A. Furube, Y. Ohga, A. Shnpo, S. Suga, K. Sayama, H. Sugihara, and H. Arakawa, *J. Phys. Chem. B*, 2003, **107**, 597-600.
24. S. Ito, T. N. Murakami, P. Comte, P. Liska, C. Grätzel, M. K. Nazeeruddin and M. Grätzel, *Thin Solid Films*, 2008, **516**, 4613-4619.
25. H. Imahori, Y. Matsubara, H. Iijima, T. Umeyama, Y. Matano, S. Ito, M. Niemi, N. V. Tkachenko and H. Lemmetyinen, *J. Phys. Chem. C.*, 2010, **114**, 10656-10665.

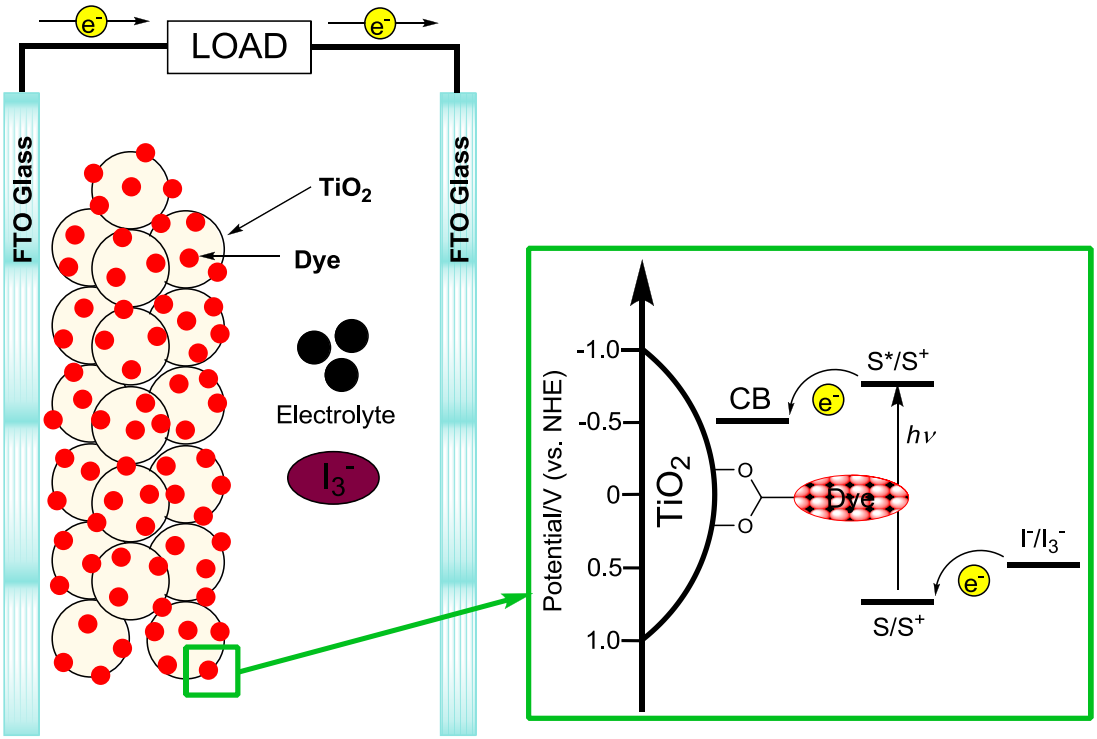

Figure 1. Construction and operation of a DSSC.

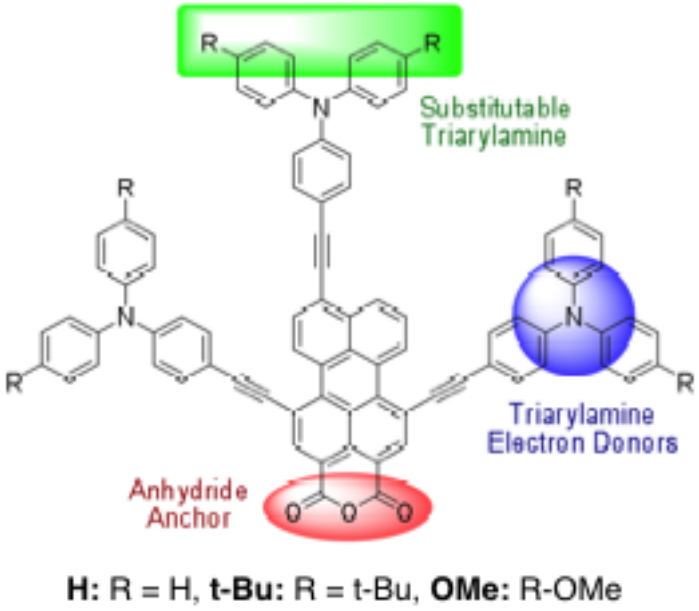

H: R = H, **t-Bu:** R = t-Bu, **OMe:** R-OMe

Figure 2. Structure of the perylenes **H**, **t-Bu**, and **OMe** used in this study.

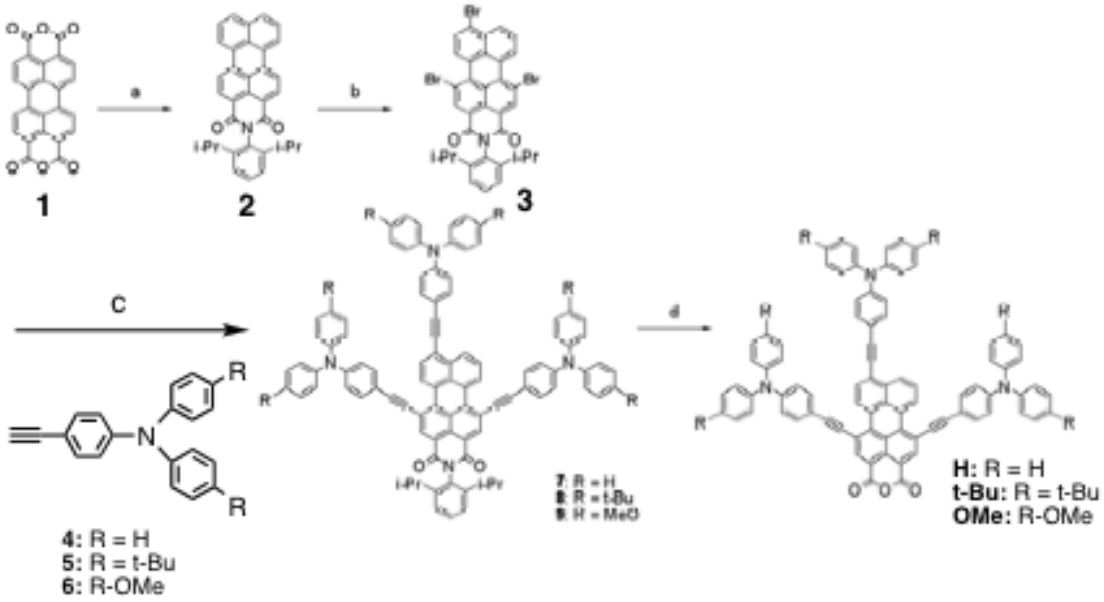

Scheme 1. Synthesis of perylene dyes **H**, **t-Bu**, and **OMe**. a) 2,6-diisopropylaniline, $Zn(OAc)_2$, quinoline/*N*,*N*-dibutylethanolamine, 230°C, b) Br_2, $CHCl_3$, reflux, c) **4-6,** $Pd(PPh_3)_4$, CuI, THF/ *N*,*N*-Diisopropylethylamine (1:1), 80°C 12h, d) KOH, *tert*-BuOH, reflux 12h.

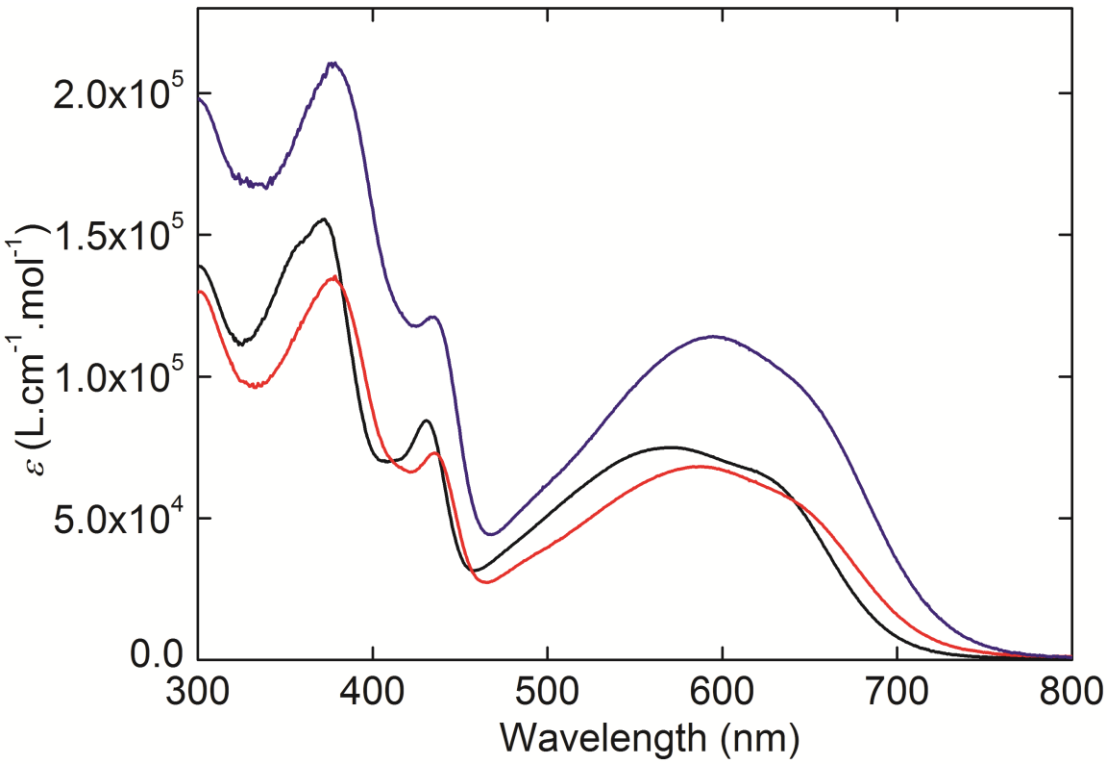

Figure 3. UV-Vis spectra of perylenes **H** (black), **t-Bu** (red), and **OMe** (blue) in CH_2Cl_2.

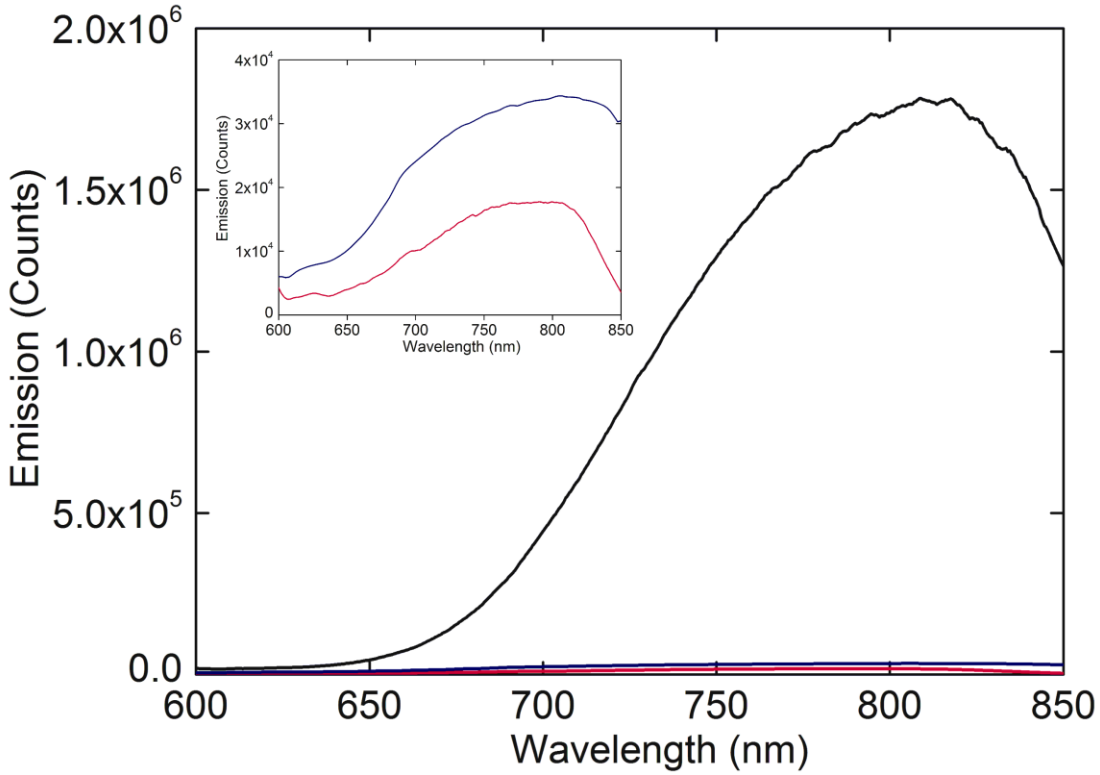

Figure 4. Fluorescence spectra of **H** (black), **t-Bu** (red), and **OMe** (blue) in CH_2Cl_2 (λ_{ex} = 573 nm). The absorbance at 573 nm was adjusted to be identical for comparison.

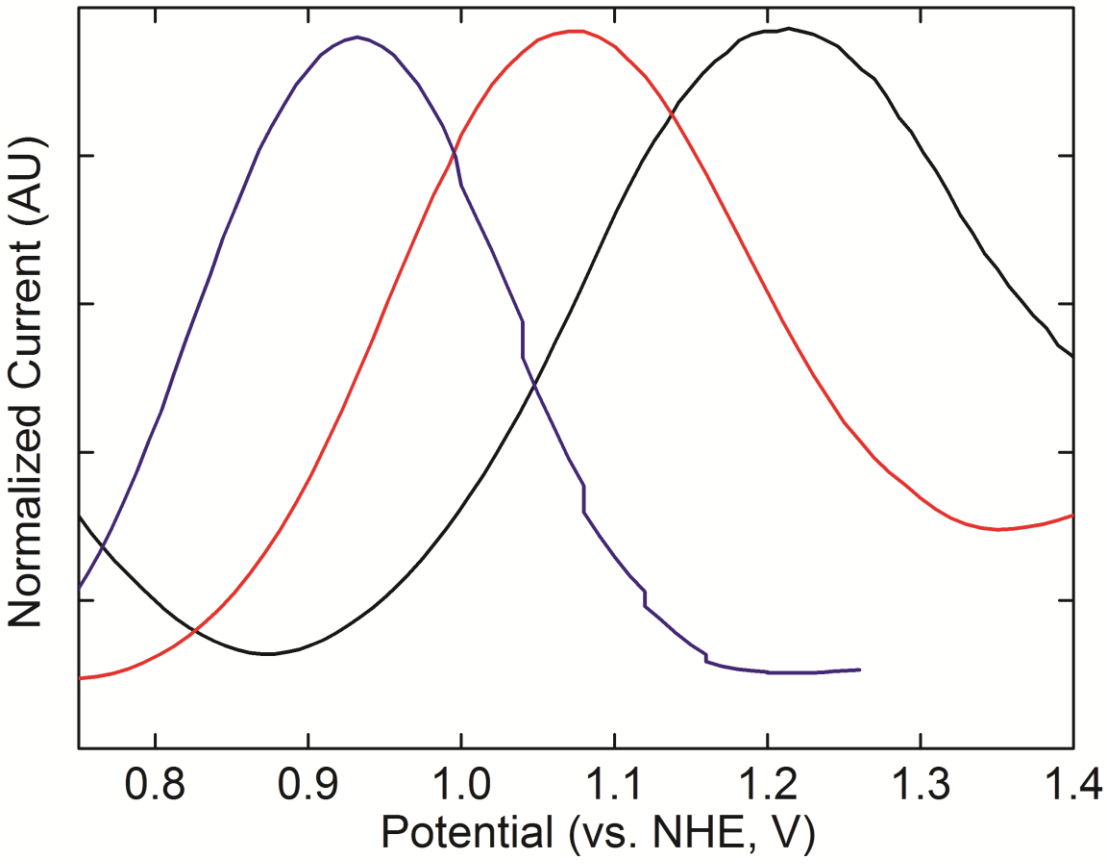

Figure 5. DPV curves of **H** (black), **t-Bu** (red), **OMe** (blue) (vs. NHE) obtained in CH_2Cl_2 containing 0.1 M Bu_4NPF_6.

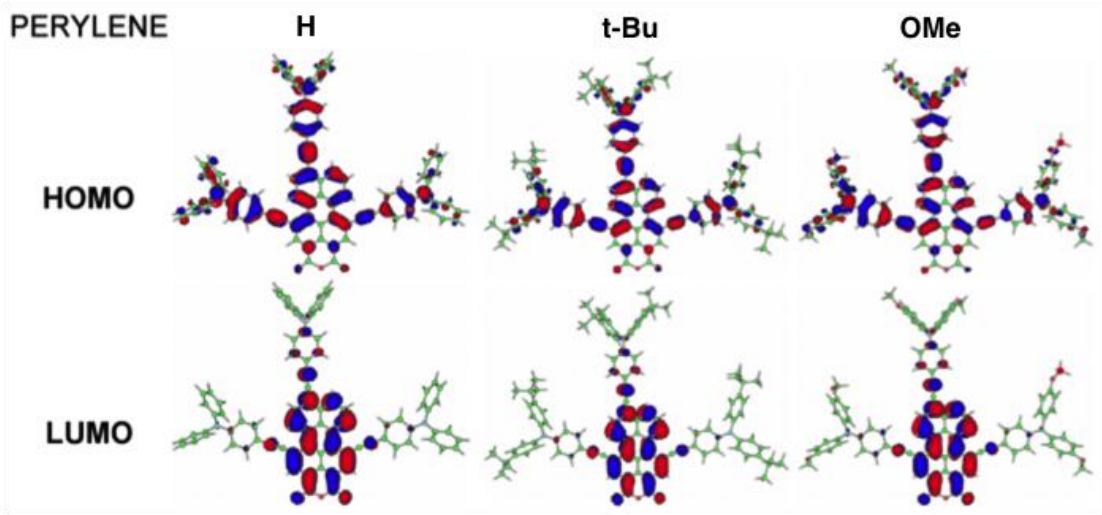

Figure 6. Frontier orbitals of perylenes **H**, **t-Bu**, and **OMe** optimized using B3LYP/3-21G level of theory.

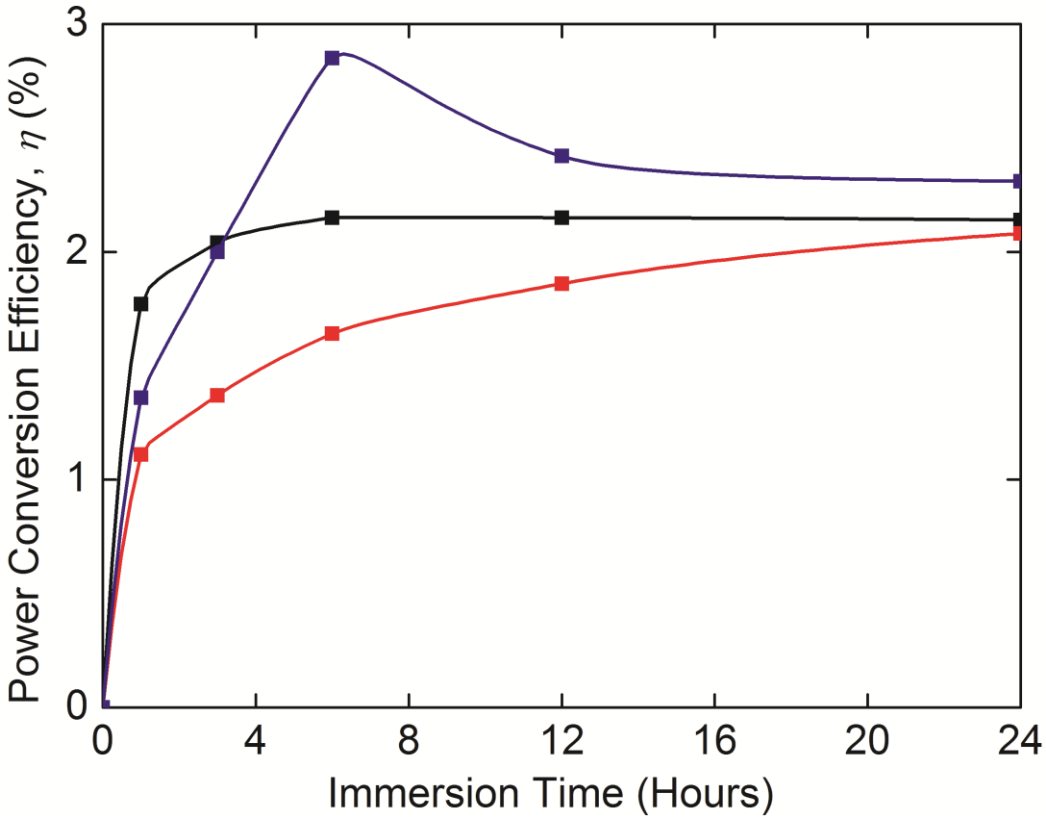

Figure 7. Immersion time profiles vs. η for perylenes **H** (black), **t-Bu** (red), and **OMe** (blue).

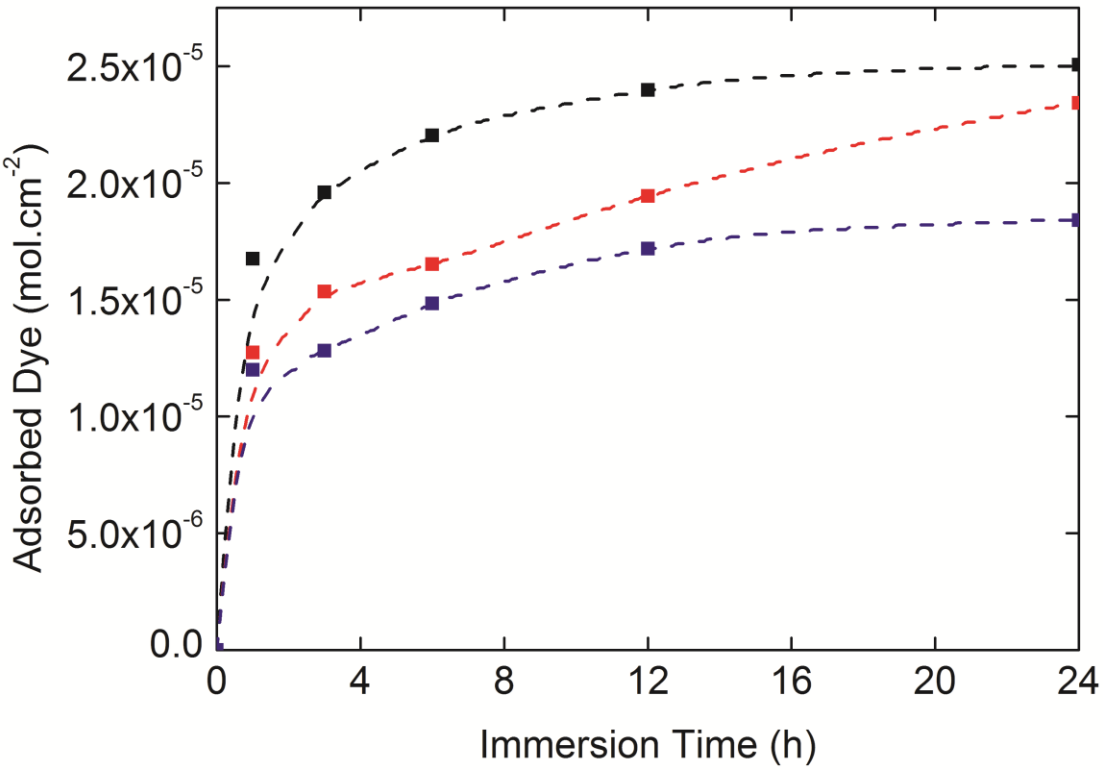

Figure 8. Plot of adsorbed dye (mol.cm^{-2}) vs. immersion time (h) for perylenes **H** (black), **t-Bu** (red), and **OMe** (blue).

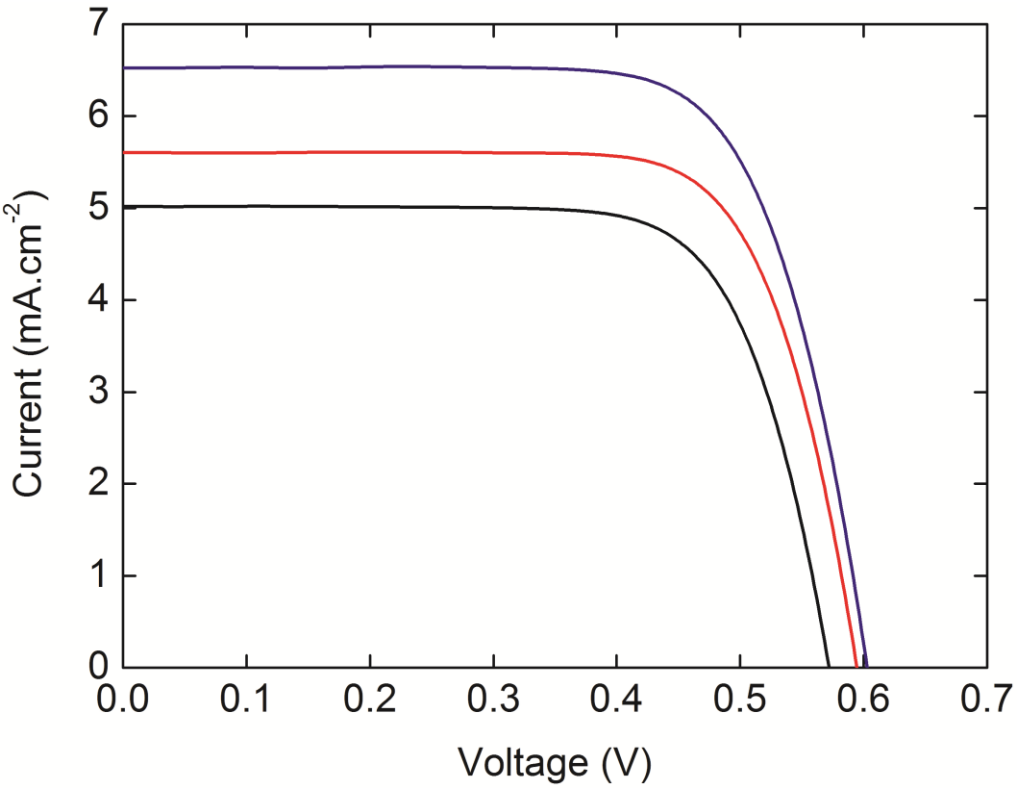

Figure 9. Photocurrent-voltage characteristics of perylenes **H** (black), **t-Bu** (red), and **OMe** (blue). Conditions: electrolyte 0.1 M LiI, 0.05 M I_2, 0.6 M 2,3-dimethyl-1-propyl imidazolium iodide and 0.5 M 4-t-butylpyridine in CH_3CN; input power AM 1.5 under simulated solar light 100 mW cm^{-2})

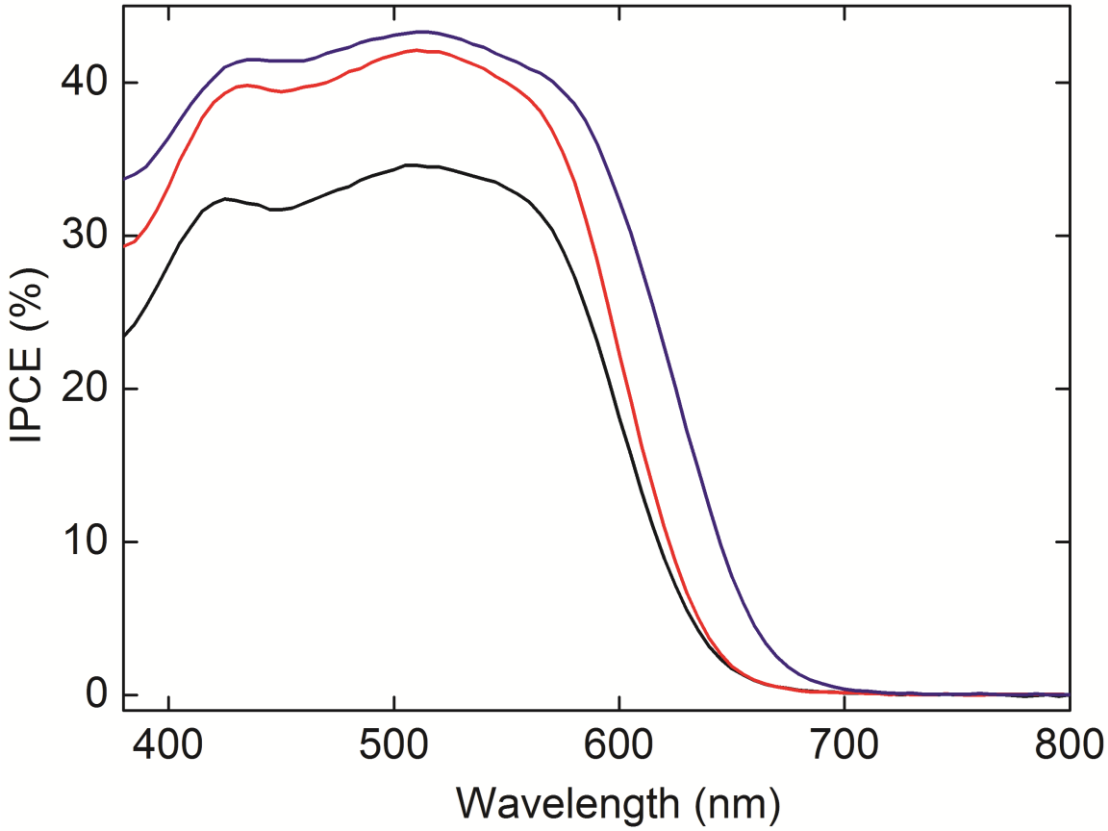

Figure 10. IPCE spectra of perylenes **H** (black), **t-Bu** (red), and **OMe** (blue).

SUPPINFO

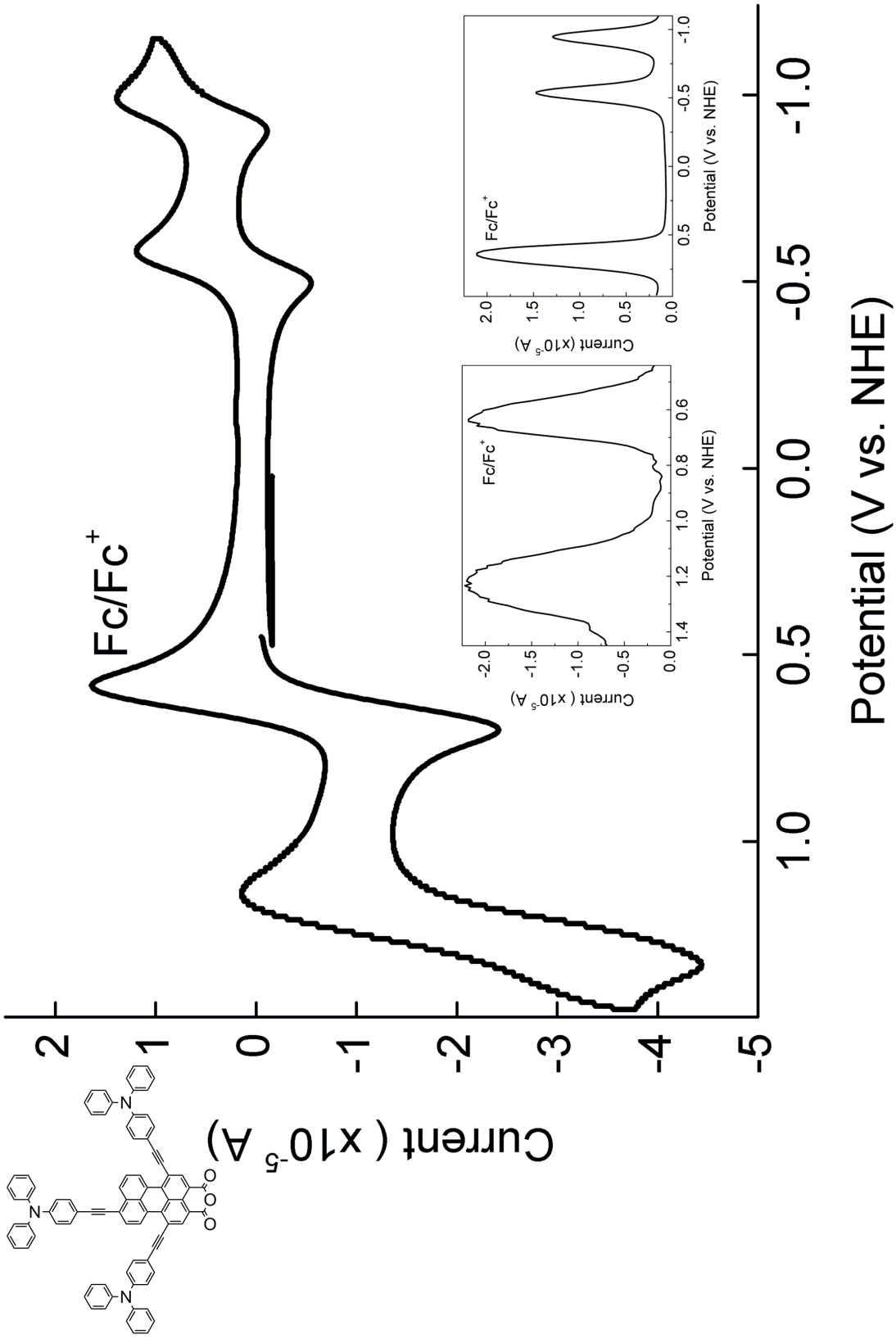

Figure S1. Cyclic voltammetry and differential pulse voltammetry curves of **H** in CH_2Cl_2 containing 0.1M Bu_4NPF_6.

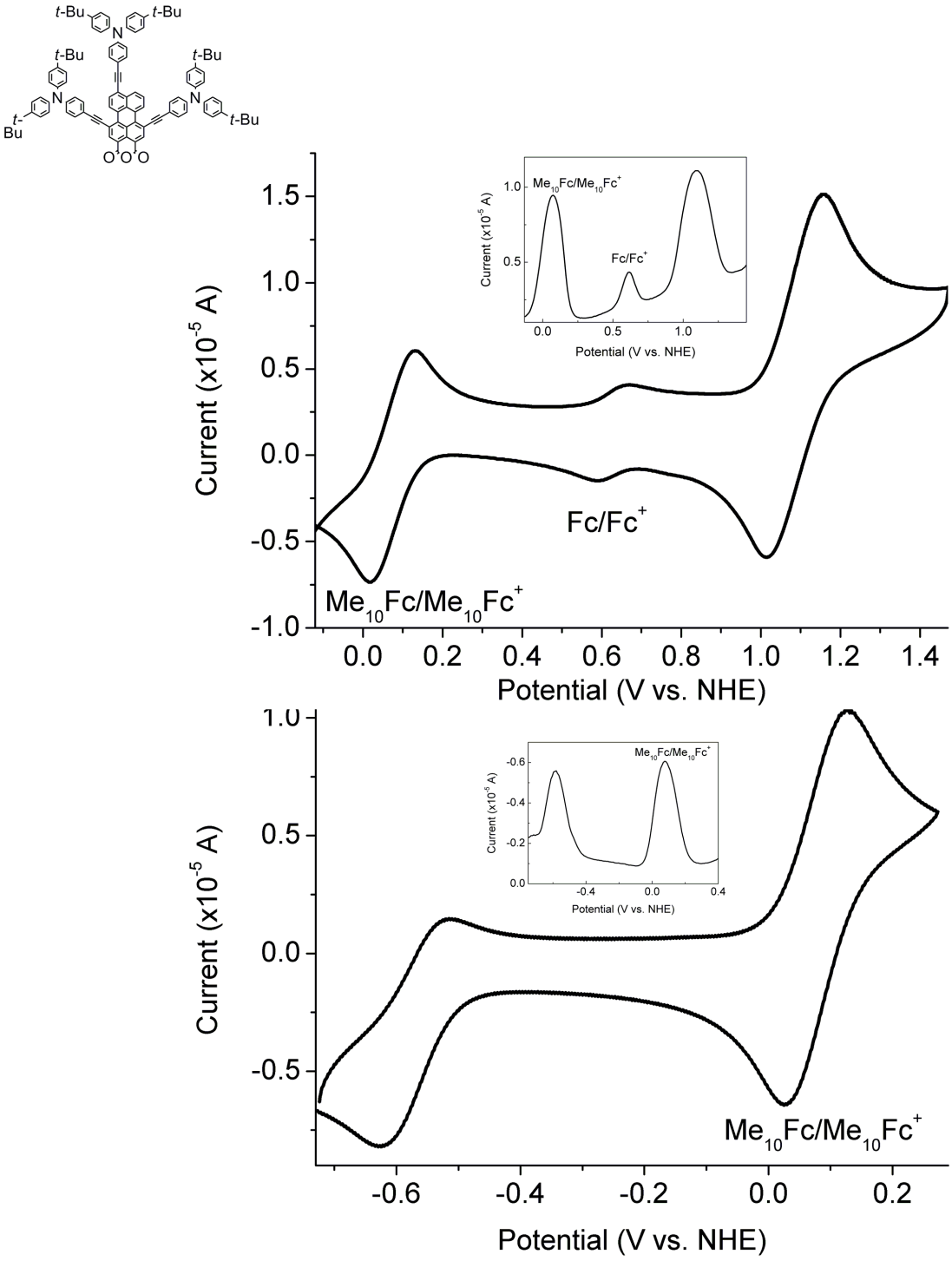

Figure S2. Cyclic voltammetry and differential pulse voltammetry curves of **t-Bu** in CH_2Cl_2 containing 0.1M Bu_4NPF_6.

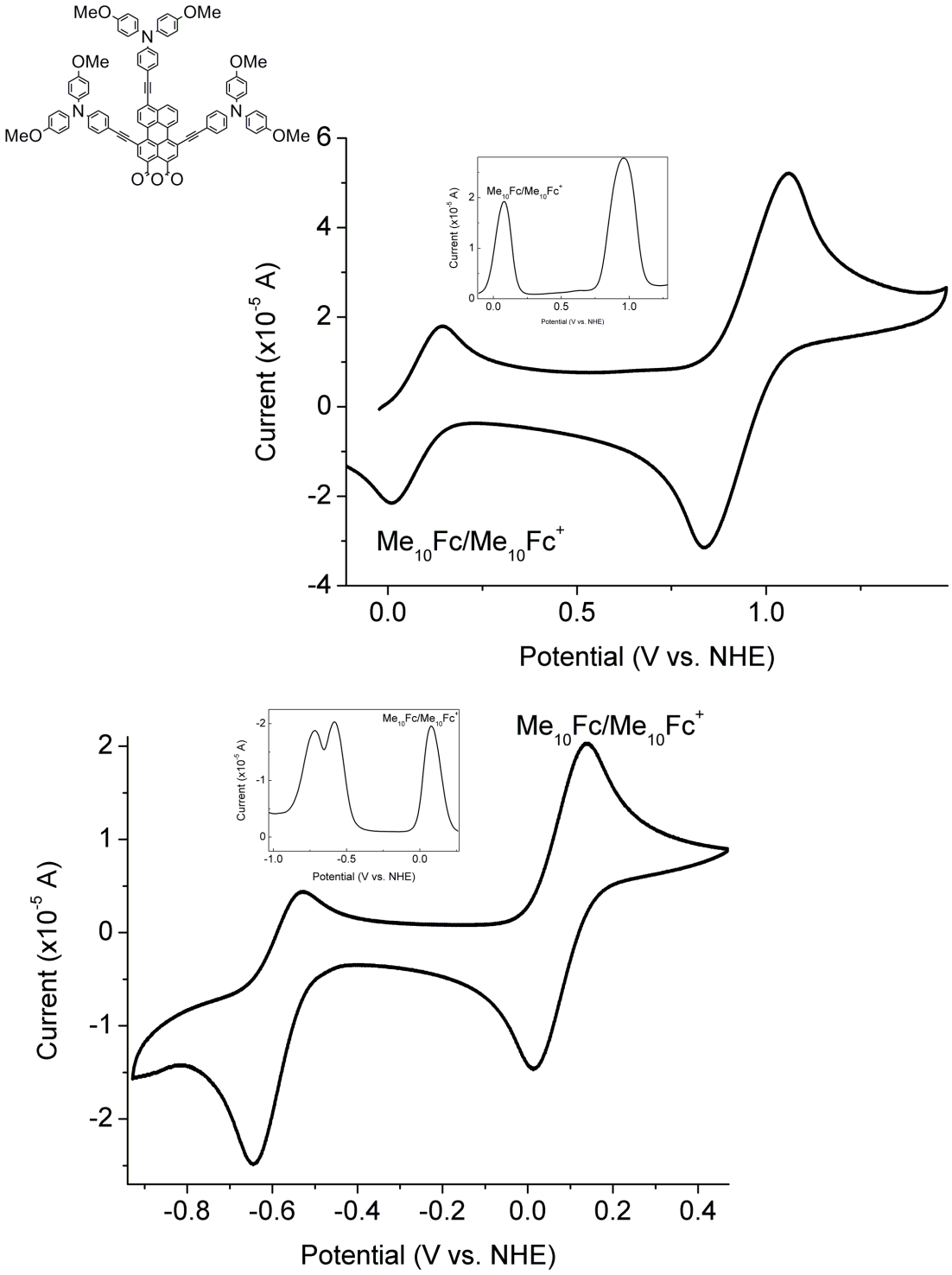

Figure S3. Cyclic voltammetry and differential pulse voltammetry curves of **OMe** in CH_2Cl_2 containing 0.1M Bu_4NPF_6.

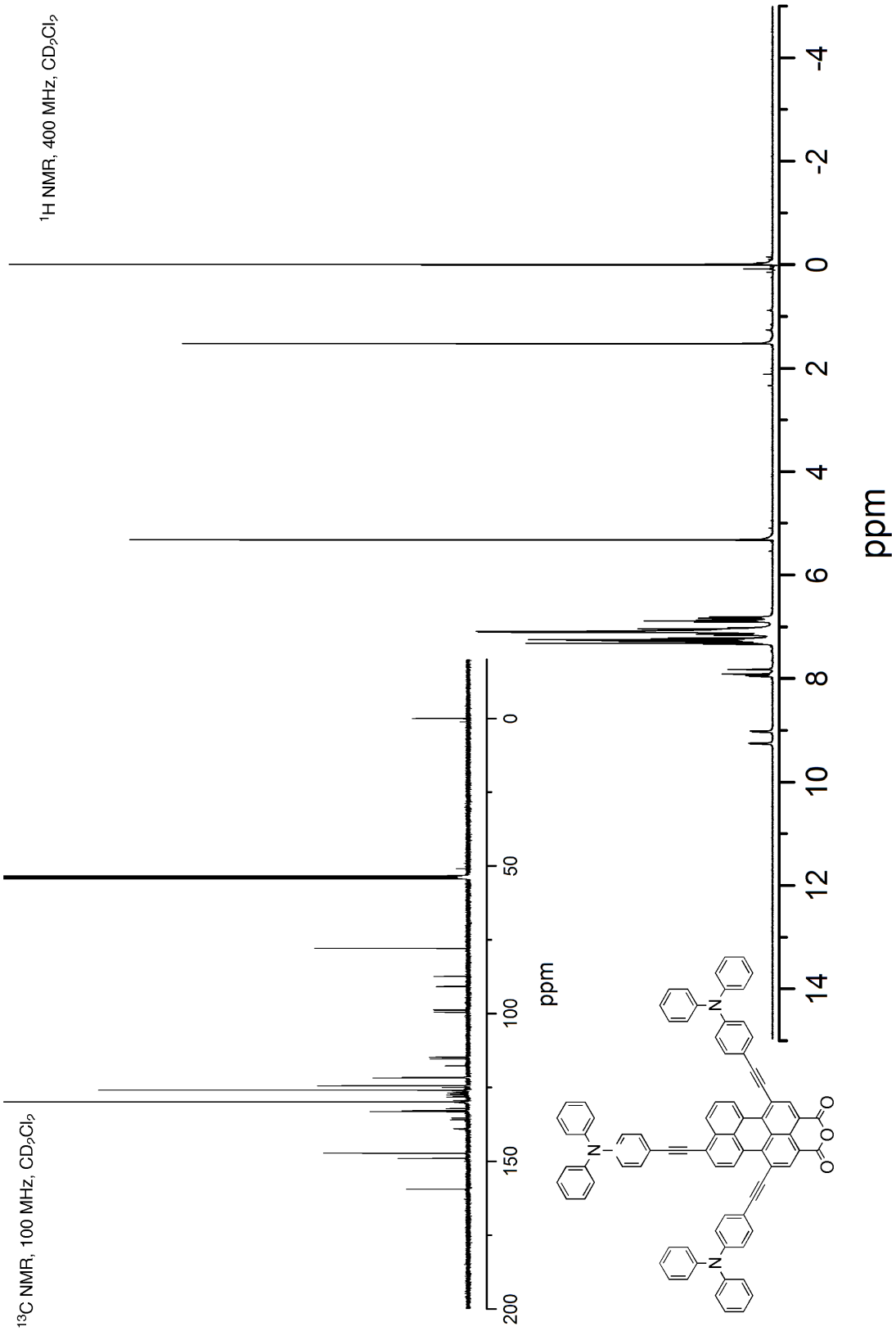

Figure S4. ^{1}H and ^{13}C NMR spectra of **H** in CD_2Cl_2.

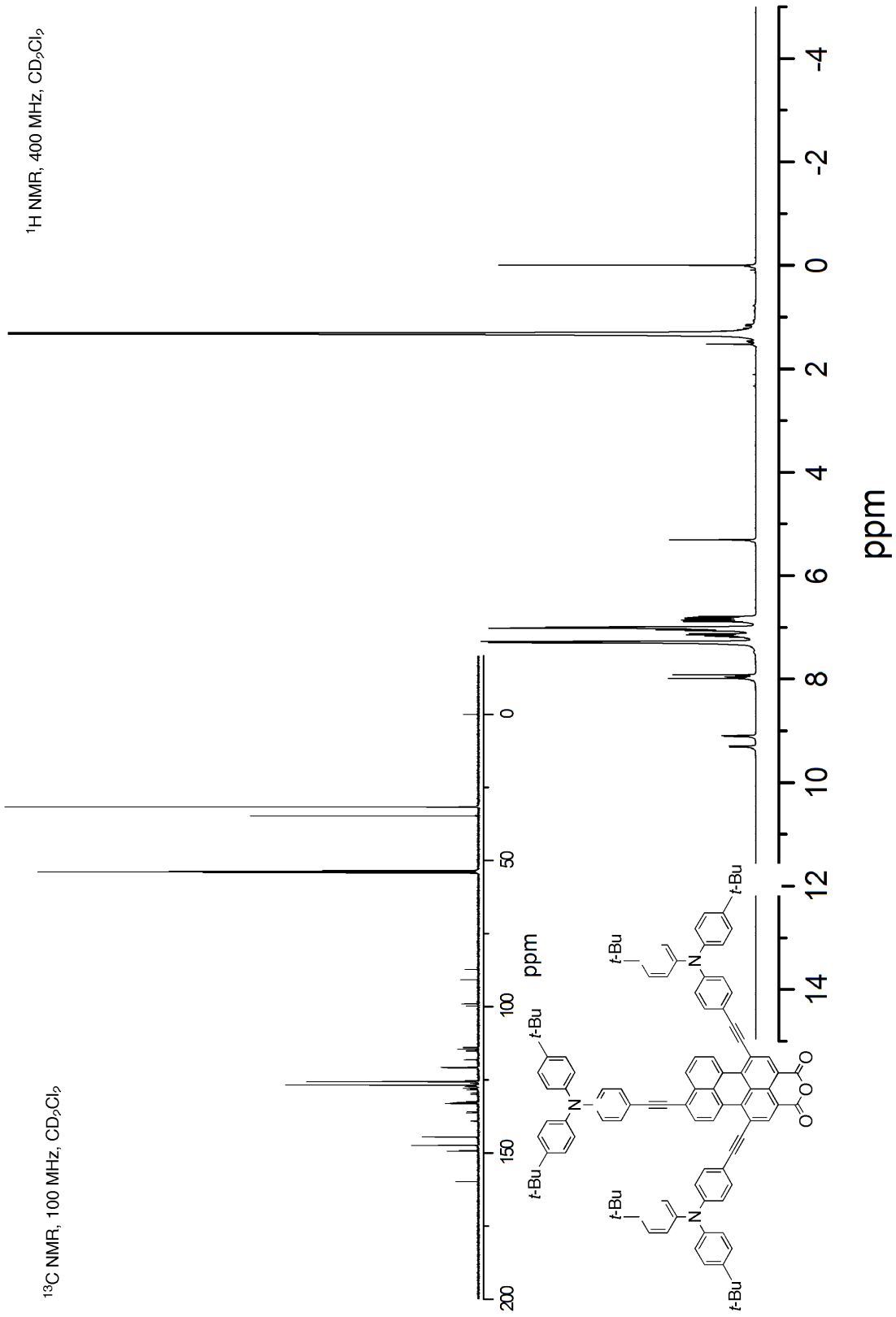

Figure S5. H and ^{13}C NMR spectra of **t-Bu** in CD_2Cl_2.

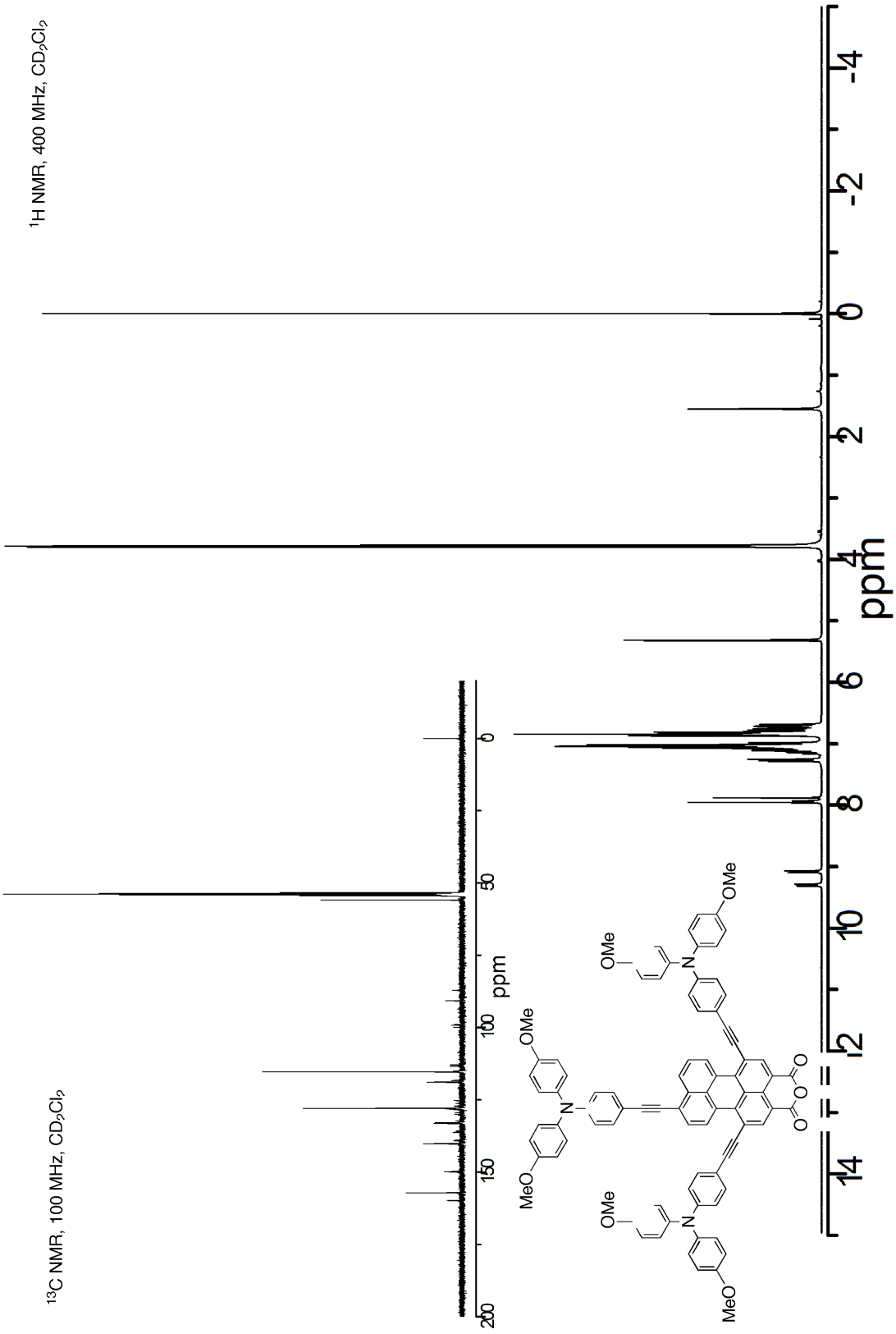

Figure S6. H and ^{13}C NMR spectra of **OMe** in CD_2Cl_2.